AD_____

Award Number: W81XWH-04-1-0891

TITLE: XIAP as a Molecular Target for Therapeutic Intervention in Prostate Cancer

PRINCIPAL INVESTIGATOR: Colin S. Duckett, Ph.D.

CONTRACTING ORGANIZATION: University of Michigan
Ann Arbor, MI 48109-1274

REPORT DATE: October 2005

TYPE OF REPORT: Annual

PREPARED FOR: U.S. Army Medical Research and Materiel Command
Fort Detrick, Maryland 21702-5012

REPORT DOCUMENTATION PAGE

Form Approved
OMB No. 0704-0188

1. REPORT DATE	2. REPORT TYPE	3. DATES COVERED
01-10-2005	Annual	23 Sep 2004 – 22 Sep 2005

4. TITLE AND SUBTITLE

XIAP as a Molecular Target for Therapeutic Intervention in Prostate Cancer

5a. CONTRACT NUMBER

5b. GRANT NUMBER
W81XWH-04-1-0891

5c. PROGRAM ELEMENT NUMBER

6. AUTHOR(S)

Colin S. Duckett, Ph.D. Steven Stain

5d. PROJECT NUMBER

5e. TASK NUMBER

5f. WORK UNIT NUMBER

7. PERFORMING ORGANIZATION NAME(S) AND ADDRESS(ES)

University of Michigan
Ann Arbor, MI 48109-1274

8. PERFORMING ORGANIZATION REPORT NUMBER

9. SPONSORING / MONITORING AGENCY NAME(S) AND ADDRESS(ES)
U.S. Army Medical Research and Materiel Command
Fort Detrick, Maryland 21702-5012

10. SPONSOR/MONITOR'S ACRONYM(S)

11. SPONSOR/MONITOR'S REPORT NUMBER(S)

12. DISTRIBUTION / AVAILABILITY STATEMENT
Approved for Public Release; Distribution Unlimited

13. SUPPLEMENTARY NOTES
Original contains colored plates: ALL DTIC reproductions will be in black and white.

14. **ABSTRACT**
We have made major progress towards the completion of the goals proposed in this award. In the first of the two Aims, we proposed to generate cell lines in which we stably suppressed XIAP using lentiviral-based RNA interference, and subsequently to constitute XIAP expression using mutants which are incapable of suppressing caspases. We have achieved this goal in PC-3 cells, and are well underway to generating similar clones in the three other cell lines we originally proposed. The first round of PC-3 derivatives have been injected into nude mice and we have exciting preliminary data supporting a role for XIAP in oncogenesis, and validating our model system for dissecting the properties of XIAP. In the second Aim, we proposed to examine XIAP expression in the TRAMP and Pten conditional transgenic murine models of prostate cancer. We have made great progress in the TRAMP system, and generated breeding colonies of Xiap-deficient, TRAMP mice. Finally, our studies to evaluate the effectiveness of a murine, XIAP-specific antisense oligonucleotide are now underway in TRAMP mice.

15. SUBJECT TERMS
Prostate Cancer; X-linked Inhibitor of Apoptosis; TRAMP; Xenograft

16. SECURITY CLASSIFICATION OF:			17. LIMITATION OF ABSTRACT	18. NUMBER OF PAGES	19a. NAME OF RESPONSIBLE PERSON
a. REPORT	b. ABSTRACT	c. THIS PAGE			USAMRMC
U	U	U	UU	25	19b. TELEPHONE NUMBER *(include area code)*

Table of Contents

Introduction

This progress report has been revised to address the comments of the reviewer, as follows:

1. The list of manuscripts and presentations has been removed, as requested.
2. We have provided a bulleted list of key research findings, with scientific descriptions that will allow the reader to review the progress of project milestones.
3. We thank the reviewer for informing us that the contract number and not the log number of the grant should be cited in publications, and will ensur that this happens in the future.
4. As requested, we have appended publications that were supported by this grant.
5. We have provided more detail to allow the reader to evaluate the actual extent of progress made toward the Statement of Work. In addition, we have presented data where relevant.

The X-linked inhibitor of apoptosis (XIAP) protein is highly expressed in prostate cancer, and has generated intense interest as a potential molecular target. The prevailing theory in the field is that the tumor-promoting effects of XIAP are due to its ability to inhibit caspases, the central effectors of apoptosis; however, the central hypothesis of our research is that this property of XIAP is relatively unimportant for the oncogenesis-supporting function of XIAP. Rather, we proposed that other XIAP-mediated activities, such as the ability to activate caspase-independent signaling pathways, are more critical for this aspect of XIAP function.

Body

We have made significant progress towards completing the tasks outlined in the original Statement of Work, as summarized below:

SPECIFIC AIM 1. To dissect and evaluate the contributions of the distinct caspase inhibitory and signaling functions of XIAP in the development of prostate cancer.

In this aim we proposed to use lentiviral-mediated RNA interference to generate clones of prostate cancer lines lacking XIAP. We proposed to subsequently reintroduce mutants of XIAP variously lacking either the caspase-inhibitory or E3 ubiquitin ligase activity of XIAP. We have made very significant progress in this area. Of the four cell lines proposed (PC-3, DU145, LNCaP and MDA PCa2b), we have initially focused on one line, PC-3, and for this particular line we have successfully 'replaced' endogenous XIAP with these mutants. We do not anticipate any major technical difficulties in the generation of the three additional cell line derivatives. In the case of PC-3, we have completed our first line of xenograft injections, and tumor burden analysis. While our data look exciting, we do not yet have sufficient numbers to be statistically significant, but this work is moving quickly.

a) Generation of prostate cancer lines in which XIAP levels have been suppressed through lentiviral-delivered, RNA interference using short hairpin RNAs. This experimental sub-aim has been highly successful. The replication-defective FG12 lentivirus system proposed in our application has proven to be highly effective and we have been able to suppress XIAP levels to virtually undetectable levels in all cell lines tested to date. Germane to the goals of this project, we have focused initially on the PC-3 line, which we have found to be highly tumorigenic in xenografts. As shown in Figure 1, we have successfully generated a number of clonal PC-3 variants the exhibit little or no expression of XIAP, as determined by immunoblot.

It has now become standard practice in the field, as well as a prerequisite for publication, to generate derivatives in this manner using distinct shRNA hairpin sequences targeting different loci of the gene in question, in order to control for potential non-specific effects. We

have also made progress in identifying such sequences, and are in the process of making similar lentiviruses. Additionally, we originally focused on the use of the PC-3 line, because this was existing in the laboratory, we are now extending these studies to an additional androgen-independent line (DU145) and two androgen-dependent lines (LNCaP and MDA Pca2b) as detailed in our original proposal.

b) Reconstitution of XIAP-suppressed prostate cancer-derived cell lines with mutants of XIAP lacking caspase-binding or E3 ubiquitin ligase activity. Consistent with the aims of our proposal, we have taken the PC-3 derivative cells lacking endogenous XIAP, and re-introduced variants which are impervious to the suppressive effects of the shRNA (due to the introduction of silent codon changes into the XIAP coding sequence), and have additionally created a panel of such cell lines using expression vectors encoding XIAP in which the caspase inhibitory properties of XIAP are abrogated. As can be seen in Figure 2, these proteins express to at least wild-type levels, and in several cases to even higher levels. As originally proposed, we have also attempted to generate reconstituted cell lines in which the E3 ubiquitin ligase activity of XIAP has been abrogated, through the generation of a single residue mutation (H467A). Interestingly, despite multiple attempts, we have been unable to generate such stable lines with this variant (Figure 2), although transient expression of H467A can readily be achieved. This finding suggests that the RING-mutated version of XIAP might be functioning as a dominant negative to inhibit growth of cells, and this is clearly an observation that requires further study.

c) Tumorigenicity studies of XIAP-suppressed prostate cancer cell lines. As detailed above and in our original proposal, we have begun these studies using the androgen-independent PC-3, and consequently these studies are more advanced at present. We have used our PC-3 derivative cell lines in xenograft implantation studies, using athymic nude mice, and compared tumor burden derived from parental cells, cells in which XIAP levels have been suppressed through shRNA, and control cells. As shown in Figure 3, the cells lacking XIAP are greatly impaired in their ability to form tumors, and this serves both to validate the model and set the stage for the next set of experiments where cells will be examined that have been reconstituted with variants of XIAP lacking caspase inhibitory activity (see below).

d) Tumorigenicity studies of reconstituted cell lines expressing XIAP variants. These studies are in progress. The first xenograft implantations have been injected, but the data are too early to draw statistically relevant conclusions.

SPECIFIC AIM 2. To validate XIAP as a novel target for the treatment of prostate cancer, using established transgenic and conditionally targeted murine models.

2.1 Analysis of the rate of tumor progression in *Xiap*-deficient mice.

a) Examination of Xiap expression profiles in TRAMP and Pten conditionally deficient mice. In this sub-aim, we proposed firstly to confirm a previous report that Xiap expression is enhanced in the TRAMP, and ultimately Pten-conditional, murine models of prostate cancer. This is complete in the case of the TRAMP model, and have demonstrated a significant enhancement of Xiap during disease progression. Since TRAMP mice were already available at our institution and within our lab, we have begun by focusing on this strain, and primarily due to the availability of Pten-targeted mice form Jackson Laboratories, we have yet to begin these studies on the Pten conditional mice. Thus, these studies are still in progress.

b) Evaluation of the contribution to tumorigenesis of XIAP using *Xiap*-targeted mice. The second goal of this sub-aim was to breed our Xiap-deficient mice to TRAMP (and ultimately Pten-conditional) mice, and examine tumor burden. This section of work is well underway, and we have had the opportunity to couple the study in a collaboration with the imaging group at the University of Michigan to examine mice using whole-body MRI scanning techniques (Figure 4). The preliminary data, some of which are shown in Figure 5, while not statistically significant, suggest a trend in which Xiap-null mice develop tumors either at the same rates as littermate controls, or potentially slightly earlier. Our range of analysis is between ~16 and 40 weeks of age. We are also in the process of examining earlier stage mice, and are evaluating histologically prostate samples from the animals, as well as liver and lung sections to look for possible changes in micrometastases between Xiap-deficient and littermate control TRAMP mice. These studies are therefore in progress.

2.2 Use of murine models of prostate cancer evaluate the effectiveness of XIAP-specific antisense strategies.

In this sub-aim, we proposed to use stabilized antisense oligonucleotides designed and validated specifically to target murine Xiap, in a study to examine their effects on tumor development in TRAMP and Pten-conditional murine prostate cancer models. The dosage regimen for this reagent (in parallel with a scrambled control oligonucleotide) is underway in our first round of TRAMP transgenic mice. From our preliminary studies, we have found good evidence that adminstration of Xiap-specific antisense elicits an anti-tumor response. However, we have also observed a number of non-specific effects that are deleterious to the mice using the scrambled non-specific control. We are therefore working with the group providing the antisense reagents (Aegera, Inc.) to further understand the nature of these non-specific effects. In summary, these studies are in progress.

Figures

Figure 1. Stable depletion of XIAP in PC3 human prostate carcinoma cells by RNA interference. Short hairpin RNA sequences specifically targeted to XIAP (A) or a control were cloned into an FG12-derived lentiviral vector. Lentiviruses were packaged in 293T cells and incubated with PC3 cells as shown in (B); infected cells are illuminated in red due to the presence of dsRed2. Infected cells were purified by FACS, and XIAP levels were assessed by immunoblot, as shown in (C).

Figure 2. Growth of PC3 cells in immunodeficient mice. Athymic nude mice (Charles River Laboratories) were subcutaneously injected with 5×10^6 PC3 cells/ injection site. Four mice were injected bilaterally with XIAP shRNA cell lines in the left flank (red triangles) and control shRNA lines in the right flank (green circles); the expression of XIAP in these lines is shown in the left panel. One mouse was injected bilaterally with parental PC3 cells (blue dashes). Tumor growth was estimated based on orthogonal caliper measurements, using $mass = a \times b^2 / 2$, where a and b are the longest and shortest measurements, respectively.

Figure 3. Expression of XIAP mutants in XIAP-depleted cells. Site-directed mutagenesis of XIAP created silent mutations in the cDNA sequence to render its expression resistant to RNA interference, as shown in the left panel. Mutant XIAP was cloned into the lentiviral vector system, and cell lines with stable depletion of XIAP were infected. XIAP protein was detected in cell lystates by immunoblot (right panel).

Figure 4. Abdominal MRI of TRAMP mice. Representative MRI cross-section scans of XIAP wt and XIAP$^{-/-}$ mice crossed into the TRAMP prostate cancer model. Prostate size (yellow arrow) is shown at 21 weeks and 25 weeks of age.

Figure 5. Overall survival and disease-free survival of TRAMP mice. TRAMP mice were bred with XIAP wt or XIAP$^{-/-}$ mice. Thirteen XIAP$^{-/-}$ offspring and eleven XIAP wt littermate controls were monitored by abdominal palpation and MRI. (A) Age at onset of palpable abdominal tumor. (B) Age at time of death.

Figure 1

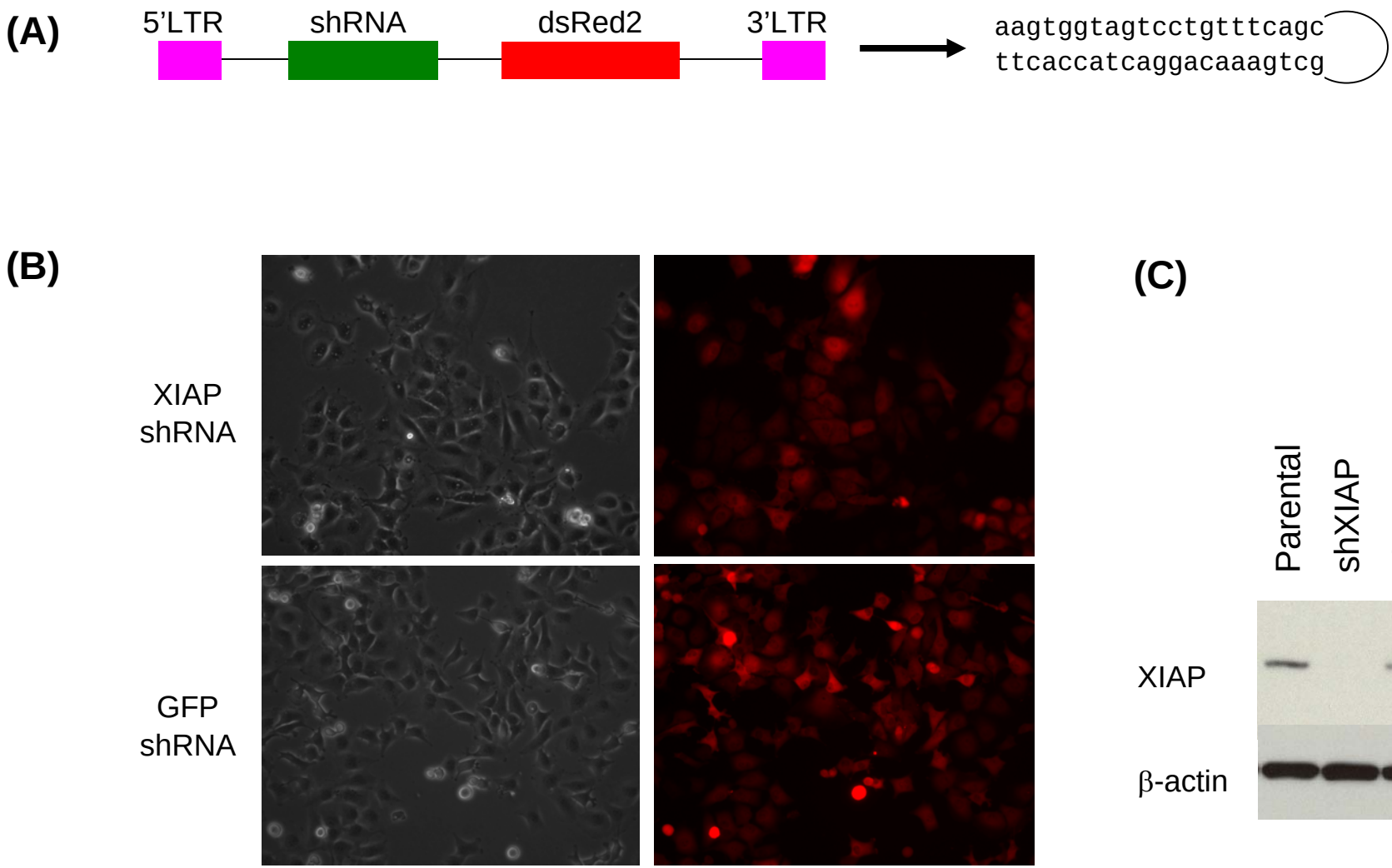
(A)
5'LTR
shRNA
dsRed2
3'LTR
aagtggtagtcctgtttcagc
ttcaccatcaggacaaagtcg
(B)
XIAP
shRNA
GFP
shRNA
(C)
Parental
shXIAP
shGFP
XIAP
β-actin

Figure 2

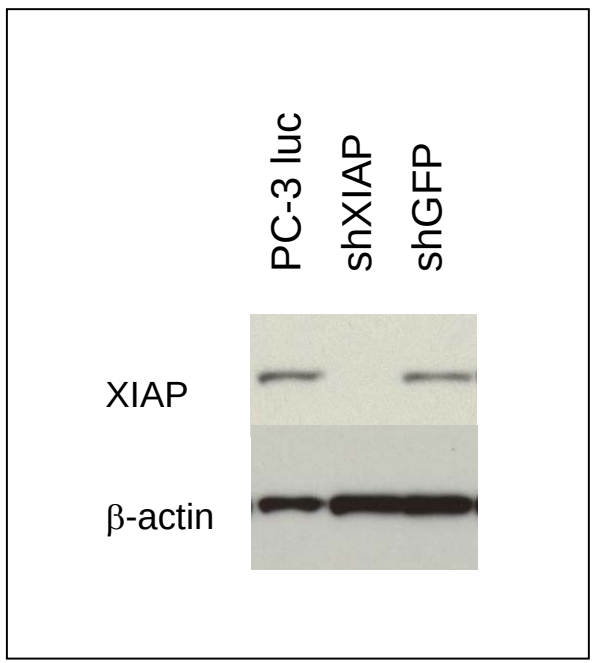
PC-3 luc
shXIAP
shGFP
XIAP
β-actin

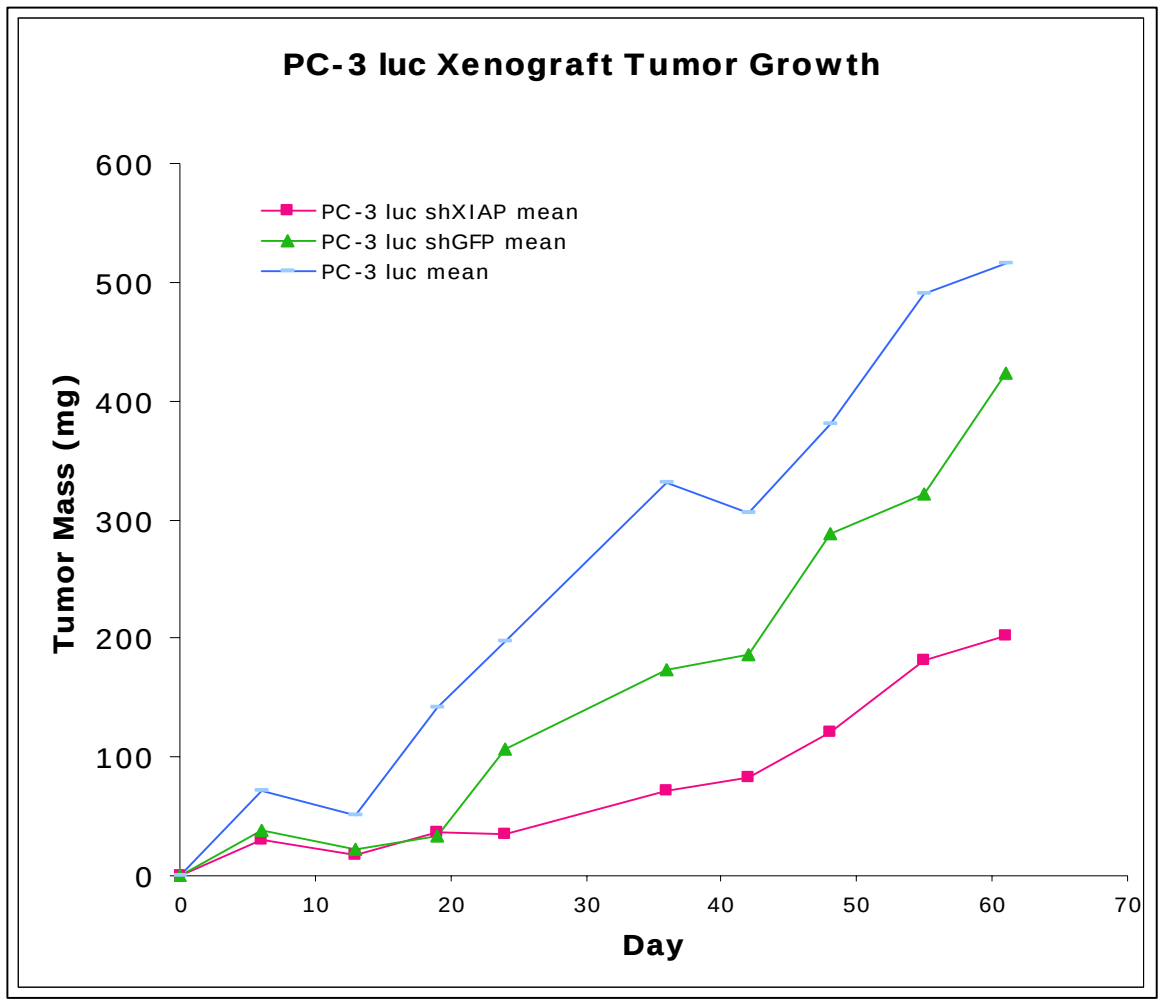
PC-3 luc Xenograft Tumor Growth
PC-3 luc shXIAP mean
PC-3 luc shGFP mean
PC-3 luc mean
Tumor Mass (mg)
600
500
400
300
200
100
0
0
10
20
30
40
50
60
70
Day

Figure 3

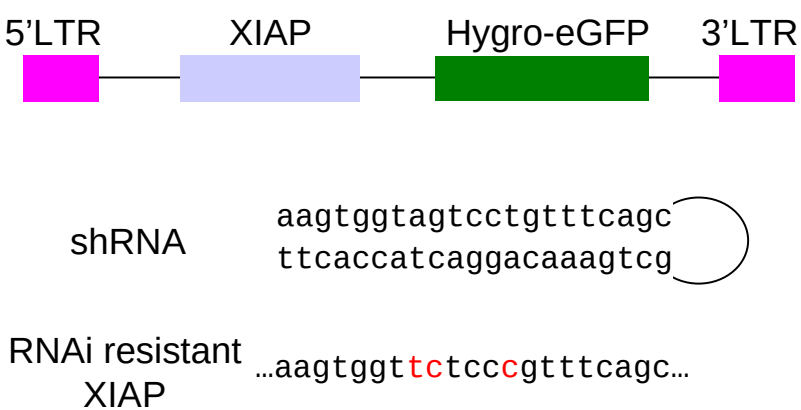
5'LTR
XIAP
Hygro-eGFP
3'LTR
shRNA
aagtggtagtcctgtttcagc
ttcaccatcaggacaaagtcg
RNAi resistant XIAP
…aagtggttctcccgtttcagc…

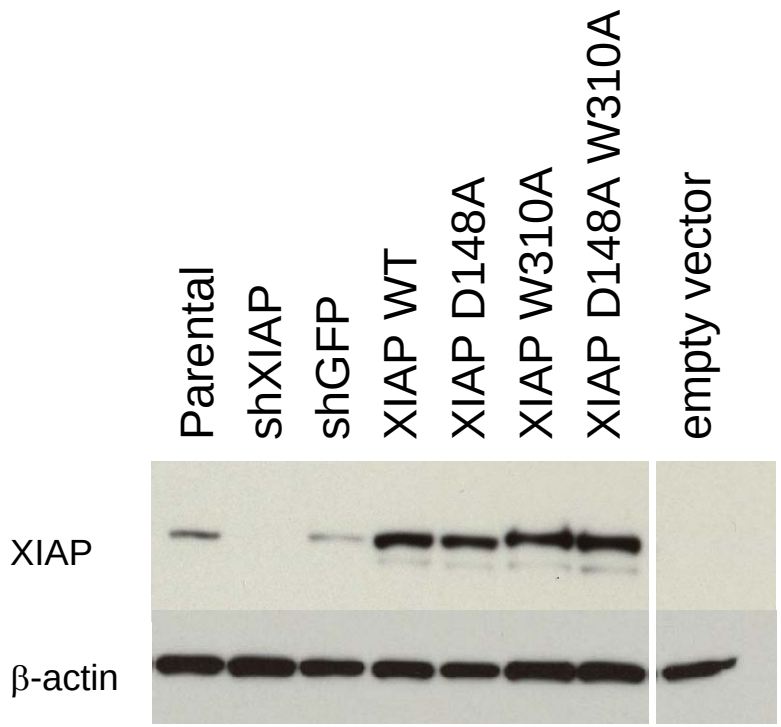
Parental
shXIAP
shGFP
XIAP WT
XIAP D148A
XIAP W310A
XIAP D148A W310A
empty vector
XIAP
β-actin

Figure 4

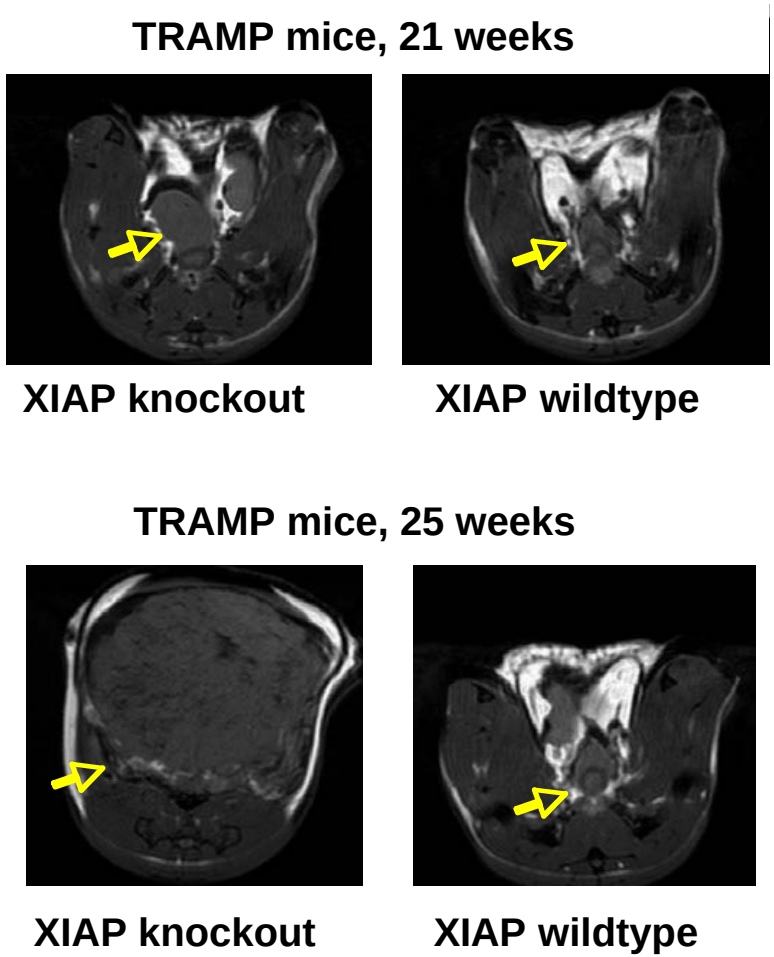
TRAMP mice, 21 weeks
XIAP knockout
XIAP wildtype
TRAMP mice, 25 weeks
XIAP knockout
XIAP wildtype

Figure 5

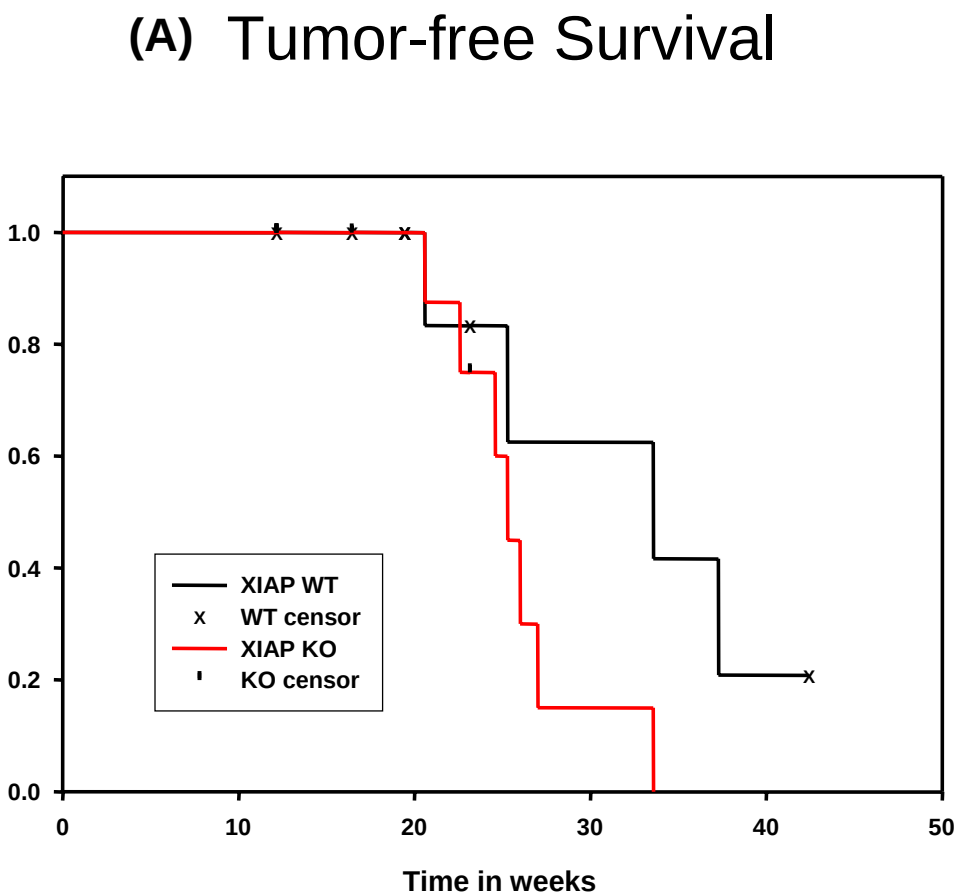
(A) Tumor-free Survival
1.0
0.8
0.6
0.4
0.2
0.0
0
10
20
30
40
50
Time in weeks
XIAP WT
WT censor
XIAP KO
KO censor

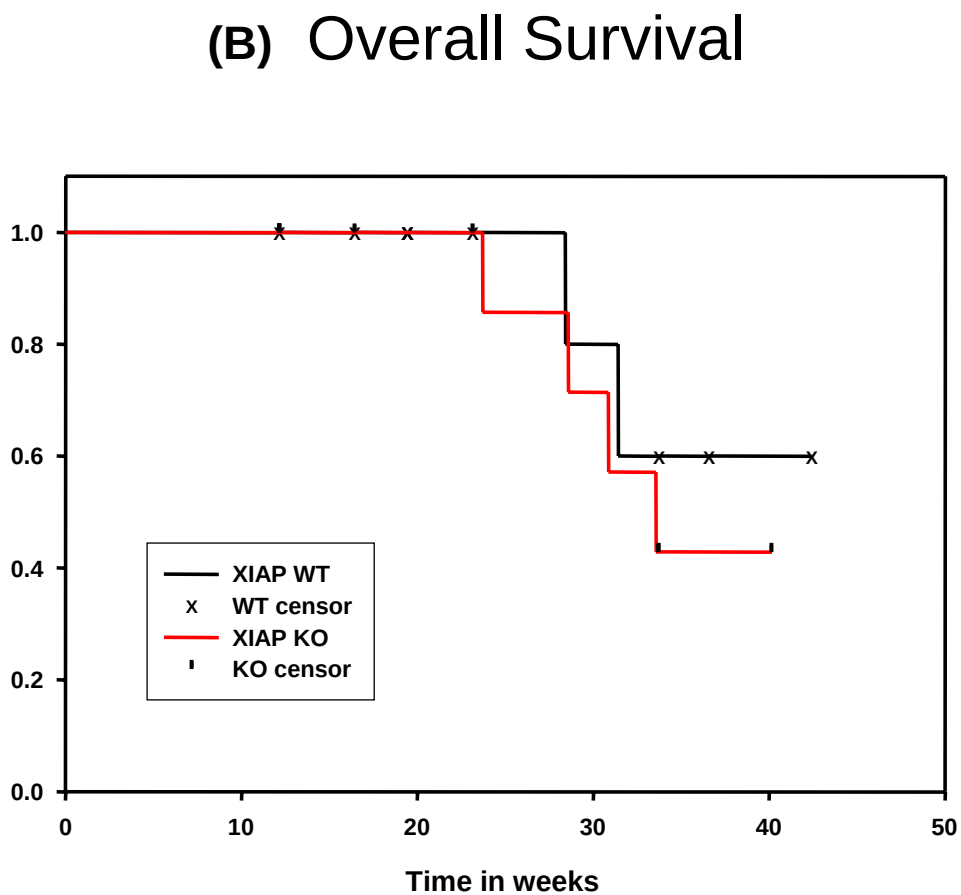
(B) Overall Survival
1.0
0.8
0.6
0.4
0.2
0.0
0
10
20
30
40
50
Time in weeks
XIAP WT
WT censor
XIAP KO
KO censor

Key Research Accomplishments

- Generated PC-3 prostate cancer cell line derivatives lacking XIAP.
- Generated retroviral expression vectors to reintroduce XIAP variants into PC-3 cells.
- Performed preliminary xenograft lines with XIAP-suppressed prostate cancer lines.
- Bred XIAP-deficient mice to TRAMP mice.
- Performed whole-body MRI and tumor burden studies on TRAMP/XIAP-deficient mice

Reportable Outcome

The following manuscripts have been published in this reporting year, and cite this grant:

Burstein, E., Hoberg, J.E., Wilkinson, A.S., Rumble, J.M., Csomos, R.A., Komarck, C.M., Maine, G.N., Wilkinson, J.C., Mayo, M.W. and **Duckett, C.S.** COMMD proteins: a novel family of structural and functional homologs of MURR1. *J Biol. Chem* **280:**22222-22232 (2005).

Conclusions

We have made significant progress with these studies. The potentially most significant technical hurdles have been overcome. Most significant of these was the established of a protocol to use lentiviral delivery to both inhibit endogenous XIAP (using RNA interference) and reconstitute the same cells with specific XIAP mutants. This entailed significant protocol development, which included the generation of lentiviral mutants expression either green fluorescent protein (GFP) or dsRed 2, and a flow cytometric-based sorting of cellular populations expressing both the RNA interfering hairpin and the reconstituting transgene. In addition, through a great collaboration with Didi Robins' group, we have been very successful in bring the TRAMP murine model of prostate cancer into the lab, and in developing the tools and techniques to follow these mice. In summary, we believe we are well on track with these studies.

Appendix

Burstein, E., Hoberg, J.E., Wilkinson, A.S., Rumble, J.M., Csomos, R.A., Komarck, C.M., Maine, G.N., Wilkinson, J.C., Mayo, M.W. and **Duckett, C.S.** COMMD proteins: a novel family

THE JOURNAL OF BIOLOGICAL CHEMISTRY Vol. 280, No. 23, Issue of June 10, pp. 22222–22232, 2005
Printed in U.S.A.

COMMD Proteins, a Novel Family of Structural and Functional Homologs of MURR1*[S]

Received for publication, February 22, 2005, and in revised form, March 11, 2005
Published, JBC Papers in Press, March 30, 2005, DOI 10.1074/jbc.M501928200

Ezra Burstein‡§, Jamie E. Hoberg¶, Amanda S. Wilkinson‖, Julie M. Rumble‖, Rebecca A. Csomos‖, Christine M. Komarck‡, Gabriel N. Maine‡, John C. Wilkinson‖, Marty W. Mayo‖, and Colin S. Duckett‡‖**

From the Departments of ‡Internal Medicine and ‖Pathology, University of Michigan Medical School, Ann Arbor, Michigan 48109-0602, ¶Department of Biochemistry and Molecular Genetics, University of Virginia, Charlottesville, Virginia 22908, and §Gastroenterology Section at the Ann Arbor Veterans Affairs Medical Center, Ann Arbor, Michigan 48105

MURR1 is a multifunctional protein that inhibits nuclear factor κB (NF-κB), a transcription factor with pleiotropic functions affecting innate and adaptive immunity, apoptosis, cell cycle regulation, and oncogenesis. Here we report the discovery of a new family of proteins with homology to MURR1. These proteins form multimeric complexes and were identified in a biochemical screen for MURR1-associated factors. The family is defined by the presence of a conserved and unique motif termed the COMM (copper metabolism gene MURR1) domain, which functions as an interface for protein-protein interactions. Like MURR1, several of these factors also associate with and inhibit NF-κB. The proteins designated as COMMD or COMM domain containing 1–10 are extensively conserved in multicellular eukaryotic organisms and define a novel family of structural and functional homologs of MURR1. The prototype of this family, MURR1/COMMD1, suppresses NF-κB not by affecting nuclear translocation or binding of NF-κB to cognate motifs; rather, it functions in the nucleus by affecting the association of NF-κB with chromatin.

NF-κB is a dimeric complex formed by members of a highly conserved family of proteins that share a defining motif designated the Rel homology domain (RHD).[1] Through transcriptional regulation of many gene products, NF-κB participates in a number of biological processes including innate and adaptive immune responses, programmed cell death, cell cycle progression, and oncogenesis (1–6). Additionally, by its ability to regulate transcription of various viral genomes including human immunodeficiency virus-1 (HIV-1) (7–10), NF-κB also participates in viral cycle progression.

Studies into the regulation of NF-κB activation have largely focused on the role of cytoplasmic sequestration of the NF-κB complex as a mainstay level of control. In most cells NF-κB is localized in the cytoplasm through the interaction of the complex with members of the IκB family (11). These proteins contain ankyrin repeats that allow their interaction with NF-κB and mask the nuclear localization signal present in the RHD. Phosphorylation of IκB by a multimeric kinase known as the IκB kinase complex targets these proteins for ubiquitination and proteasomal degradation (3, 12). This allows the translocation of NF-κB to the nucleus where it binds to cognate DNA sequences present in an array of gene promoters.

MURR1 is a recently identified factor that has been shown to participate in two apparently distinct activities, regulation of the transcription factor NF-κB and control of copper metabolism (13). Mutations in *MURR1* are responsible for copper toxicosis in an inbred canine strain (Bedlington terriers) (14), and an interaction between MURR1 and the copper transporter ATP7B (15) has been recently reported.

In addition to its role in copper metabolism in mammals, more recent studies implicate MURR1 in the regulation of the transcription factor NF-κB (13, 16). MURR1 was found to be a broad inhibitor of NF-κB, affecting κB-responsive transcription from endogenous and viral promoters including the HIV-1 enhancer (16). Through this effect, MURR1 can function as a factor that limits HIV-1 replication in resting $CD4^+$ lymphocytes.

Here we report the discovery of a family of proteins structurally and functionally related to MURR1. These factors contain a unique and defining domain termed the COMM (copper metabolism gene MURR1) domain, and thus, these proteins have been named COMM domain-containing or COMMD proteins. Similar to MURR1/COMMD1, several of these factors associate with NF-κB and inhibit its transcriptional activity. In addition, we find that COMMD proteins form heteromeric complexes that are mediated by the COMM domain. The prototype of the family, MURR1/COMMD1, exerts its ability to inhibit κB-mediated transcription without affecting nuclear translocation but through nuclear regulation of NF-κB. We show here that MURR1/COMMD1 is recruited to chromatin of a κB-responsive promoter upon NF-κB activation and negatively regulates the association of RelA to chromatin. Therefore, this work identifies a novel family of factors that regulate NF-κB-mediated transcription by controlling the occupancy of NF-κB on chromatin.

* This work was supported in part by the University of Michigan Biological Scholars Program, Department of Defense Idea Award PC040215 and National Institutes of Health Grant GM067827 (to C. S. D.), by an American Gastroenterological Association Research Scholar Award, a Merit Review Entry Program Award, and a Veterans Education and Research Association of Michigan Award (to E. B.), by NCI, National Institutes of Health Grants K01CA78595, R01CA104397, and R01CA095644 (to M. W. M.), and by T32 CA09676 (to J. C. W.). The costs of publication of this article were defrayed in part by the payment of page charges. This article must therefore be hereby marked "*advertisement*" in accordance with 18 U.S.C. Section 1734 solely to indicate this fact.

[S] The on-line version of this article (available at http://www.jbc.org) contains a supplemental figure and table.

** To whom correspondence should be addressed: Med. Sci. I, Rm. 5315, 1301 Catherine, Ann Arbor, MI 48109-0602. Tel.: 734-615-6414; Fax: 734-615-7012; E-mail: colind@umich.edu.

[1] The abbreviations used are: RHD, Rel homology domain; EGFP, enhanced green fluorescence protein (GFP); TAP, tandem affinity purification; GST, glutathione *S*-transferase; TNF, tumor necrosis factor; MS, mass spectroscopy; RT, reverse transcription; EMSA, electrophoretic mobility shift assay; ChIP, chromatin immunoprecipitation; RNAi, RNA interference; siRNA, small interfering RNA; HIV-1, human immunodeficiency virus-1.

EXPERIMENTAL PROCEDURES

Plasmids—The plasmids pEBB, pEBG, pEBB-MURR1-Flag and pEBB-MURR1-GST, pEBB-T7-IκB-αS.D., 2κB-luc, and EGFP-p65 (kindly provided by Dr. Rainer de Martin) have been described previously (17–22). pEBB-COMMD1-GST vectors expressing exon 1, exon 2-3, and exon 1-3 were generated by PCR amplification using pEBB-MURR1-Flag as template with the boundaries outlined in Fig. 3*C*. pEBB-MURR1-TAP was constructed by subcloning MURR1 into pEBB-TAP, which was generated by PCR amplification of the coding sequence for the tandem affinity purification (TAP) tag using pBS1539 as template (23). Expression vectors for COMMD proteins in fusion with Flag and glutathione *S*-transferase (GST) (pEBB-COMMD-Flag or pEBB-COMMD-GST) were generated by PCR amplification of the coding sequences for each of these proteins. To that effect the following full-length IMAGE clones were used as templates to amplify COMMD2 through COMMD10, respectively: 4443942, 3531636, 5743903, 6644608, 1692591, 5275167, 4051246, 4333615, and 3683093. pEBG-RelA-(1–305), pEBG-RelA-(306–551), and pEBG-RelA-(1–180), pEBG-c-Rel-(1–180), pEBG-RelB-(97–267), and pEBG-p50-(1–233) and pEBG-p52-(1–212) were generated by PCR using the vectors RSV-RelA, RSV-c-Rel, RSV-RelB, RSV-p50, and RSV-p52 as templates, respectively (kindly provided by Dr. Neil Perkins) (24).

Cell Culture, Transfection, and Luciferase Assays—Human embryonic kidney 293 cells and prostate cancer and DU145 cells were obtained from ATCC. 293 cells were cultured in Dulbecco's modified Eagle's medium supplemented with 10% fetal bovine serum and L-glutamine, and DU145 cells were cultured in minimum Eagle's medium supplemented with 10% fetal bovine serum, L-glutamine, sodium bicarbonate, and pyruvate. A standard calcium phosphate transfection protocol (20) was used to transfect plasmids and siRNA oligonucleotides into 293 cells. Delivery of siRNA oligonucleotides into DU145 cells was performed using Oligofectamine (Invitrogen) as specified by the manufacturer. For luciferase reporter experiments, cells were seeded in 6-well plates and transfected with 4 μg of pEBB plasmid, and 25 ng of the reporter plasmid 2κB-luciferase. Luciferase assays were performed as described previously (25). TNF (Roche Applied Science) treatments consisted of 1000 units/ml for 12 h. For immunoprecipitation experiments cells were seeded in 10-cm plates and transfected with a total of 12 μg of plasmid. Finally, suppression of endogenous COMMD expression was achieved by transfection of 293 cells seeded in 6-well plates with 2 μg of the corresponding siRNA oligonucleotides (Qiagen).

TAP Screening—293 cells seeded in 15-cm plates were transiently transfected with pEBB-MURR1-TAP (15 μg of plasmid/plate) and 2 days later were lysed in Triton lysis buffer (25 mM HEPES, 100 mM NaCl, 1 mM EDTA, 10% glycerol, 1% Triton X-100, protease inhibitors). The lysate was supplemented with NaCl and Nonidet P-40 and applied to a chromatography column containing IgG-Sepharose beads (Amersham Biosciences). After 2 h of incubation at 4 °C the column was drained and washed with IPP150 buffer (10 mM Tris-HCl, pH^+ 8.0, 150 mM NaCl, 0.1% Nonidet P-40, protease inhibitors) and TEV cleavage buffer (10 mM Tris-HCl, pH^+ 8.0, 150 mM NaCl, 0.1% Nonidet P-40, 0.5 mM EDTA, 1 mM dithiothreitol, protease inhibitors). After incubation for 2 h at 16 °C in TEV cleavage buffer supplemented with TEV enzyme (Invitrogen), the eluate was collected and supplemented with $CaCl_2$ and IPP150 calmodulin binding buffer (10 mM Tris-HCl, pH^+ 8.0, 150 mM NaCl, 0.1% Nonidet P-40, 1 mM magnesium acetate, 1 mM imidazole, 2 mM $CaCl_2$, 10 mM β-mercaptoethanol). This was then applied to a chromatography column containing calmodulin 4B beads (Amersham Biosciences) and incubated at 4 °C for 1 h. The column was then drained and washed with IPP150 calmodulin binding buffer. After incubation at 4 °C with IPP150 calmodulin elution buffer (10 mM Tris-HCl, pH^+ 8.0, 150 mM NaCl, 0.1% Nonidet P-40, 1 mM magnesium acetate, 1 mM imidazole, 2 mM EGTA, 10 mM β-mercaptoethanol), a final eluate was collected. Proteins were precipitated by adding cold 10% trichloroacetic acid in acetone; after overnight incubation at −20 °C, the precipitate was collected by centrifugation at 4 °C (10,000 × *g* for 30 min), rinsed in 100% acetone, and allowed to air dry. These samples were then submitted to the Proteomics Centre at the University of Victoria for further processing, including tryptic digestion, high performance liquid chromatography separation, and tandem mass spectrometry (MS/MS) to determine peptide sequences.

RT-PCR and Expression Data—Total RNA was extracted from 293 cells using RNeasy (Qiagen) according to the manufacturer's instructions. Yield and purity was determined by measuring $A_{260/280}$ of RNA diluted in water. Oligonucleotides and internal probes for RT-PCR and quantitative RT-PCR of *COMMD* transcripts were designed with the use of the automated primer design tool, AutoPrime (www.autoprime.de). Detailed information about sequences and cycling parameters are available upon request. For non-quantitative RT-PCR, Titan One-Tube RT-PCR (Roche Applied Science) was used according to the manufacturer's instructions. For quantitative RT-PCR reactions, an RT reaction with 500 ng of total RNA in 25 μl was performed using random hexamers and Taqman reverse transcription reagents (Applied Biosystems). This was followed by quantitative PCR performed in the 7500 real time PCR system (Applied Biosystems). In all reactions, Taqman PCR Master Mix with the appropriate primers and probes was used. Primers and probe sets for *c-IAP2* (*BIRC3*) and *GAPDH* (glyceraldehyde-3-phosphate dehydrogenase) as an internal control were obtained from Applied Biosystems. Expression data in normal tissues were obtained from the Genomics Institute of the Novartis Research Foundation (26), downloaded, and further analyzed.

Immunoblotting and Immunoprecipitation—Cell lysates were prepared by adding Triton lysis buffer; immunoblotting and GSH precipitations were performed as previously described (19). A polyclonal COMMD1 antiserum was raised by immunizing New Zealand White rabbits. Recombinant protein, which was used as immunogen, was produced in *Escherichia coli* by expressing GST-COMMD1 using the pGEX-4T1 bacterial expression vector (Amersham Biosciences). GST-COMMD1 was purified over a glutathione-Sepharose chromatography column (Amersham Biosciences), and COMMD1 was generated by thrombin cleavage of the GST affinity tag according to the manufacturer's instructions. Antibodies against Flag (Sigma, A8592), RelA (BD Transduction Laboratories, 610868), c-Rel (Santa Cruz, sc-6955), RelB (Santa Cruz, sc-226), p50 (Upstate Biotechnology, 06–886), p52 (Upstate Biotechnology, 05–361), IκB-α (Upstate Biotechnology, 06–494), GST (Santa Cruz, sc-459), α-tubulin (Molecular Probes, A11126), and GCN5 (Santa Cruz, sc-20698) were used as indicated.

Confocal and Fluorescence Microscopy—293 cells were plated in chambered cover glass plates or 6-well plates and transfected with EGFP-p65 (25 or 50 ng/well, respectively). Morphological assays for nuclear translocation of EGFP-p65 were performed by observing cells with a Zeiss Axiovert 100 M confocal microscope before and after treatment with TNF. Representative images were obtained, and 250–400 cells were observed and scored accordingly.

Electrophoretic Mobility Shift Assay (EMSA)—293 cells were seeded in 10-cm dishes and transfected as indicated. TNF stimulation, when performed, consisted of treating cells with 1000 units/ml for 30 min before lysis. The preparation of nuclear extracts and EMSA have been described previously (24). For our studies, a double-stranded oligonucleotide encompassing a canonical κB sequence was used as probe (forward sequence, AGCTTACAAGGGACTTTCCGCTGGGGACTTTCCAGGG).

Cellular Fractionation—293 cells were plated in 10-cm plates 48 h before the procedure. Medium was aspirated, and the cells were rinsed in phosphate-buffered saline, scraped, and collected in a microcentrifuge tube. The cells were resuspended in 200 μl of buffer 1 (25 mM HEPES, 5 mM KCl, 0.5 mM $MgCl_2$, 1 mM phenylmethylsulfonyl fluoride, 1 mM dithiothreitol, and protease inhibitors). After that, 200 μl of buffer 2 were added (Buffer 1 with 1% Nonidet P-40), and the cells were incubated with constant rotation at 4 °C for 15 min. The samples were centrifuged for 1 min at 600 × *g*, and the supernatant, corresponding to the cytoplasmic fraction, was collected. The precipitated material was gently rinsed in 100 μl of buffer 3 (1:1 mixture of buffers 1 and 2). After centrifuging the samples again as before, the supernatant was collected as part of the cytoplasmic fraction. The remaining precipitated material was then treated by the addition of 500 μl of buffer 5 (25 mM HEPES, 10% sucrose, 350 mM NaCl, 1 mM phenylmethylsulfonyl fluoride, 1 mM dithiothreitol, 0.01% Nonidet P-40, protease inhibitors) and incubated with constant rotation at 4 °C for 60 min. After this, the samples were centrifuged for 10 min at 16,100 × *g*. The supernatant, corresponding to the nuclear fraction, was collected separately.

Chromatin Immunoprecipitation—Subconfluent DU145 cells were treated with TNF (1000 units/ml) before cross-linking for chromatin immunoprecipitation (ChIP) analysis. For attachment assays, 293 cells were re-plated in serum-free media on laminin-coated plates (Discovery Labware) as previously described (27). ChIP protocol and primers sequences have been previously described (28). Antibodies used in the ChIP studies include COMMD1 (described above), M2 Flag (Sigma, F3165), RNA polymerase II (Santa Cruz, SC-9001), and RelA (Upstate, 06-418).

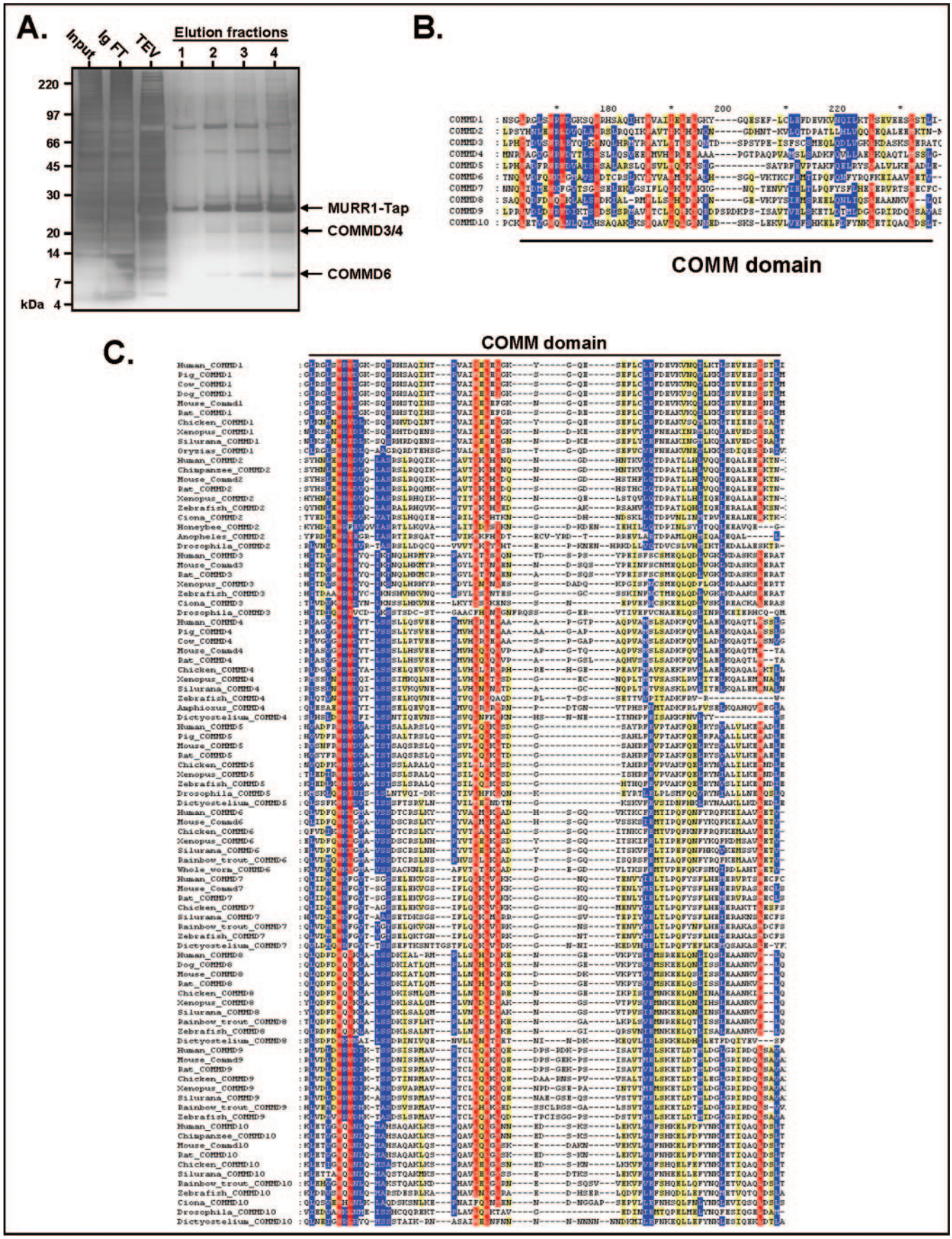

FIG. 1. *A*, identification of the COMMD protein family. Fractions obtained during TAP purification were separated by SDS-PAGE, and the gel was silver-stained. The lysate was subjected first to an immunoglobulin column, and the flow-through (*Ig FT*) and eluate (*TEV*) were collected. This eluate was further purified over a calmodulin column, and the eluates were collected in four fractions (*Elution fractions*). COMMD3, -4, and -6 were identified in the final eluate by liquid chromatography-MS/MS. *B*, human COMMD proteins. Analysis of the human protein databases using

RESULTS

Biochemical Screen for MURR1-associated Factors—To further understand the cellular activities of MURR1, a biochemical screen for associated proteins was performed based on the TAP scheme that has been previously described (23). Briefly, MURR1 in fusion with the TAP affinity tag was transiently expressed in 293 cells, and MURR1-TAP was subsequently purified from cells lysates using two sequential chromatography columns containing IgG and calmodulin beads, respectively (Fig. 1*A*). The material obtained was subjected to tryptic digestion, and the peptides generated were then identified by tandem mass spectrometry (MS/MS) after initial separation using liquid chromatography. A number of associated factors were identified, including three proteins that upon close inspection demonstrated the presence of a region with close homology to MURR1 in their carboxyl termini (Fig. 1, *A* and *B*). These factors were later designated as COMMD3, -4, and -6 (see below).

Identification of the COMMD Protein Family—After the identification of three MURR1 homologous factors in our biochemical screen, we performed an extensive search of the sequence databases for additional homologs. Through this approach we were able to identify 10 proteins in humans, including MURR1, that contain highly conserved carboxyl-terminal sequences (Fig. 1*B*). The majority of these genes were only known as open reading frames and had not been previously characterized.

Further analysis of orthologs present across multiple species demonstrated that the area of close homology in the carboxyl termini of these proteins represents a previously unrecognized, unique, and highly conserved motif (Fig. 1*C*). This leucine-rich, 70–85 amino acid long sequence is predicted to form a β-sheet. We have termed this region the copper metabolism gene MURR1 (COMM) domain.

The designation of homologs of MURR1 identified here required the generation of a new nomenclature. *Murr1* derived its name from its proximity to the *U2af1-rs1* locus in mice (mouse U2af1-rs1 region 1); however, this genomic organization is not observed in other organisms including humans. In addition, an unrelated gene that also lies in close proximity to *U2af1-rs1* has been designated *Murr2*, precluding the use of this name for MURR1 homologs (29). In consultation with the HUGO gene nomenclature committee, the term COMMD (COMM Domain containing) is proposed to designate these factors based on the shared structural domain that defines this family of proteins and has been adopted in NCBI public databases. The name COMMD1 is suggested for MURR1 as a means to standardize the nomenclature to designate this protein family and will be used hereafter.

With the exception of COMMD1, no other COMMDs have been previously described in any detail. *COMMD5* was identified as an open reading frame that is overexpressed in naturally hypertensive rats and suppressed in a number of primary tumors and cancer cell lines (30). The expressed protein localizes to the nucleus, although a direct role in transcription had not been previously demonstrated. *COMMD6* is orthologous to a mouse gene located in a region that is necessary for normal embryonic development, although it is unclear whether *COMMD6* itself is required for normal embryogenesis (31). Similarly, *COMMD3* was previously identified as a locus with close proximity to the Polycomb-group gene *Bmi-1* (32). Finally, an expressed sequence tag corresponding to *COMMD7* was found to be consistently repressed in an experimental system designed to screen for factors involved in leukemogenesis (33).

COMMD Genes Are Highly Conserved—We found that all 10 genes have been conserved throughout vertebrate evolution, as can be gleaned from orthologs found in *Silurana tropicalis, Xenopus laevis, Danio rerio*, *Oncorhynchus mykiss,* and *Oryzias latipes* (see the supplemental table). In general, mammalian sequences are about 90% conserved when compared with their human orthologs. Furthermore, lower metazoans, including insects, worms, and molds, also possess *COMMD* genes; however, none of these genes were identified in unicellular eukaryotic organisms or bacteria. Five of these genes were found in *Drosophila melanogaster* (*COMMD2*, *-3*, *-4*, *-5*, and *-10*) and *Dictyostelium discoideum* (*COMMD4*, *-5*, *-7*, *-8*, and *-10*). Overall, eight of the *COMMD* genes can be found in lower metazoans, with *COMMD1* and *COMMD9* orthologs being restricted to vertebrate species (see the supplemental figure).

Despite the presence of a conserved and defining motif in all these proteins, a significant proportion of the sequence of each COMMD protein is composed of unique regions that are divergent across members of the family. For example, human and zebrafish COMMD1 are 72% conserved, whereas human COMMD1 and COMMD10 are only 34% conserved when regions outside the COMM domain are included in the comparison (data not shown).

COMMD Genes Are Widely Expressed—Given that COMMD proteins were initially identified as COMMD1-associated factors in 293 cells, we first investigated the pattern of expression of human *COMMD* genes in this cell line. To this end, we designed primers for RT-PCR of each one of these genes including in each case one primer that was selected at an exon-exon junction. This strategy minimizes the possibility of spurious amplification from contaminating genomic DNA because such junctions are generated only after splicing. In addition, the potential for mispriming against the intronic boundary was taken into account in the design. With this algorithm we identified primers for all 10 human *COMMD* genes, with the amplicon size and position of exon-exon primers indicated in Fig. 2*A*. Using these primers and total RNA extracted from 293 cells we were able to amplify the appropriate size products for each of the *COMMD* genes (Fig. 2*B*). Template-lacking negative controls did not amplify these products (data not shown). This indicated that 293 cells express all *COMMD* genes, a fact that was also confirmed by publicly available expression data (not shown here).

Next, the level of *COMMD* expression in multiple tissues was analyzed using data available from the Genomics Institute of the Novartis Research Foundation. Utilizing oligonucleotide arrays, expression levels for more than 44,000 mRNA transcripts across 79 human tissues were determined (26). This raw data were downloaded, and the corresponding probes for most *COMMD* genes (with the exception of *COMMD6*) were identified. Expression levels in 13 selected tissues were further analyzed and are presented in Fig. 2*C*. As shown, *COMMDs* are

BLAST allowed for the identification of six additional proteins with sequence homology to MURR1. A partial alignment of all 10 human COMMD proteins is shown, demonstrating a region of higher conservation (COMM domain). The accession numbers for the 10 human mRNA sequences are NM_152516, AY542158, AY542159, AY542160, NM_014066, AY542161, AY542162, AY542163, AY542164, and AY542165, corresponding to COMMD1–10, respectively. The degree of conservation of each amino acid residue among these sequences is indicated based on Dayhoff PAM 250 scoring matrices (*red*, 90% conserved; *blue*, 70% conserved; *yellow*, 50% conserved). *C*, alignment of 91 COMMD proteins from multiple species across the COMM domain. All protein sequences spanning through the COMM domain were aligned using the ClustalV algorithm, and this alignment was then refined using the SAM program. The resulting alignment was then annotated using the GeneDoc program. The degree of conservation of each amino acid residue among these sequences is indicated based on Dayhoff PAM 250 scoring matrices as before.

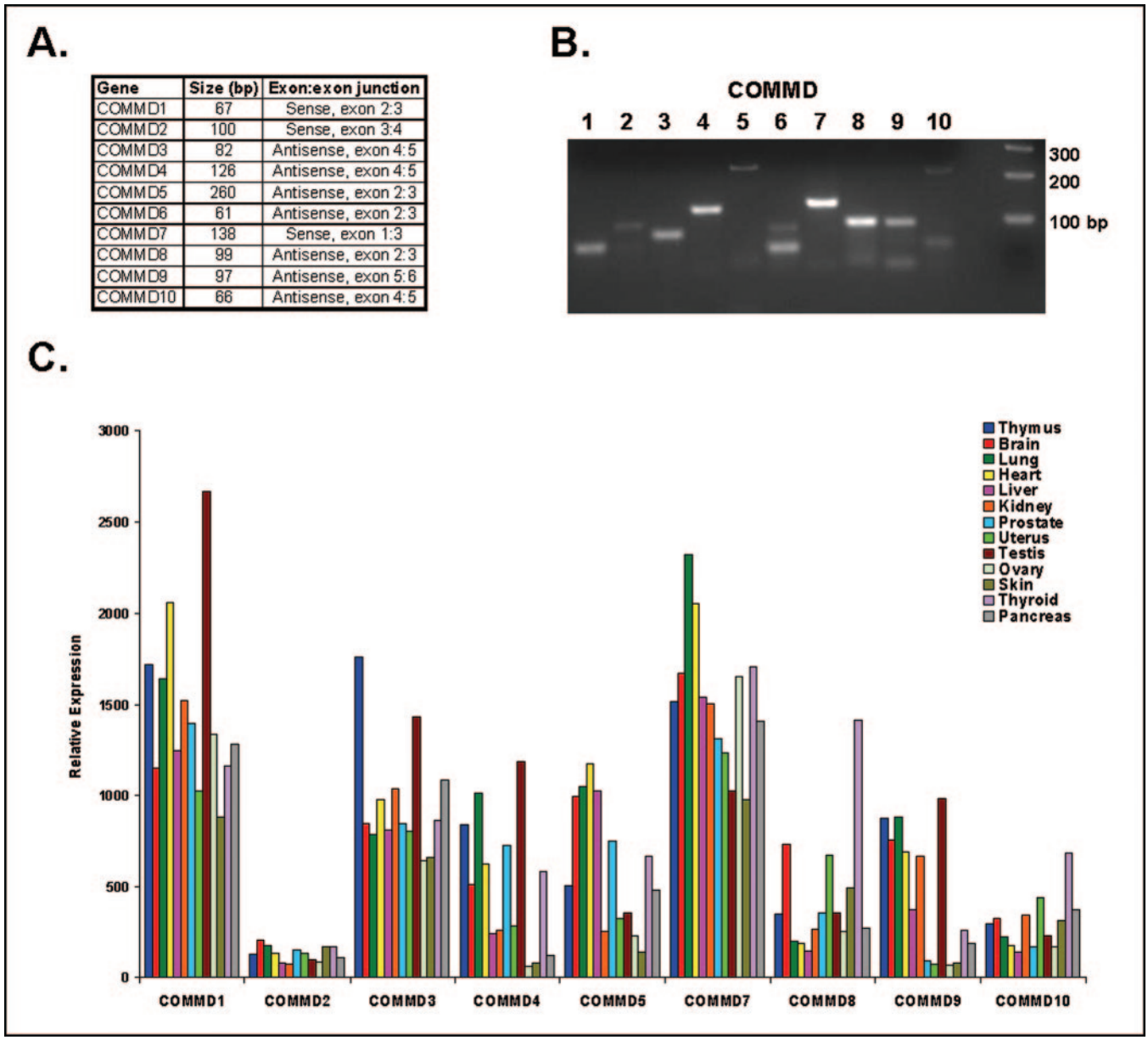

Gene	Size (bp)	Exon:exon junction
COMMD1	67	Sense, exon 2:3
COMMD2	100	Sense, exon 3:4
COMMD3	82	Antisense, exon 4:5
COMMD4	126	Antisense, exon 4:5
COMMD5	260	Antisense, exon 2:3
COMMD6	61	Antisense, exon 2:3
COMMD7	138	Sense, exon 1:3
COMMD8	99	Antisense, exon 2:3
COMMD9	97	Antisense, exon 5:6
COMMD10	66	Antisense, exon 4:5

FIG. 2. *A*, amplicon size and position of mRNA-specific primers utilized for RT-PCR. *B*, *COMMD* genes are expressed in 293 cells. Using the primer sets described, RT-PCR was performed with total RNA extracted from 293 cells serving as template. The presence of amplified products of the proper sizes was determined by agarose gel electrophoresis as shown here. *C*, expression of *COMMD* genes in 13 normal tissues. Levels of mRNA expression were determined using oligonucleotide microarrays.

widely expressed in human tissues, but the relative abundance of any given *COMMD* mRNA is different across the samples. For example, whereas *COMMD1* expression is highest in the testis, *COMMD3* is the highest expressed in the thymus, *COMMD7* in the lung, and *COMMD8* in the thyroid. Conversely, any given tissue has a complement of *COMMD* genes that demonstrate highest expression, and these subsets are not identical in each case (data not shown).

COMMD1 Can Associate with Other COMMD Proteins—COMMD3, -4, and -6 were initially identified biochemically by their ability to interact with COMMD1. Therefore, the ability of all the members of the family to interact with COMMD1 was evaluated. Each of the 10 COMMD proteins was fused to GST and expressed in 293 cells. COMMD-GST fusion proteins were then precipitated from cell lysates with glutathione-Sepharose beads, and the recovered material was immunoblotted for endogenous COMMD1 (Fig. 3*A*). COMMD1–8 and COMMD10 could readily precipitate endogenous COMMD1; COMMD9 also co-associates with COMMD1 but to a lesser extent (not shown here). These experiments demonstrated that COMMD1 can interact with itself and with all other COMMD proteins, consistent with the interactions detected in the initial TAP screen.

COMMD-COMMD Protein Interactions Are Mediated by the COMM Domain—To define the domain(s) required for COMMD multimer formation, a variety of deletion constructs of COMMD1 were tested for their ability to bind COMMD1 and COMMD3. The coding regions corresponding to each exon of COMMD1 were used as boundaries in constructs expressing fusion proteins with GST (Fig. 3*B*). The hereditary canine copper toxicosis mutation described previously consists of a genomic deletion encompassing exon 2 of *COMMD1* such that the expressed open reading frame lacks 94 amino acid residues (14). This protein product was also expressed in fusion with GST and similarly tested for its ability to bind COMMD1 and COMMD3.

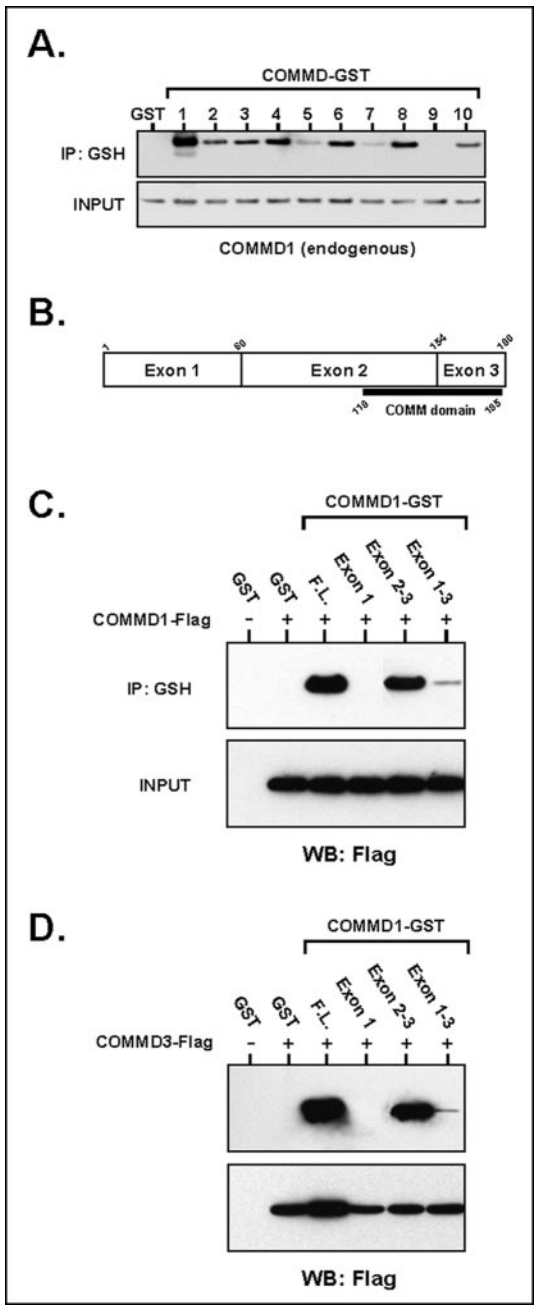

FIG. 3. *A*, COMMD-COMMD interactions. Each of the 10 COMMD proteins was expressed in 293 cells in fusion with GST and precipitated (*IP*) from cell lysates by glutathione-Sepharose beads. The presence of endogenous COMMD1 in the precipitates was determined by immunoblotting. *B*, schematic representation of COMMD1 and the amino acid residues that are the boundaries for interaction mapping experiments. *C* and *D*, the COMM domain is required for the association of COMMD proteins. COMMD1-Flag (*C*) or COMMD3-FLAG (*D*) were expressed in 293 cells along with various regions of COMMD1 in fusion with GST as indicated. COMMD1-GST was precipitated from cell lysates by glutathione-Sepharose beads and the presence of COMMD1 or -3 in the precipitates was determined by immunoblotting (*WB*) with a Flag antibody.

These fusion proteins were expressed in 293 cells and precipitated with glutathione-Sepharose beads. The ability of these fragments to support an interaction was determined by the presence of COMMD1 or COMMD3 in the precipitate (Fig. 3, *C* and *D*). The carboxyl terminus of COMMD1 (exon 2-3), which contains the COMM domain, was found to be sufficient for interactions with COMMD1 and COMMD3. The lack of the COMM domain in the exon 1-GST fusion protein abrogated binding in both cases. Furthermore, the exon 1-3 product, replicating the protein product in dogs with copper toxicosis and lacking part of the COMM domain, had a significant impairment in binding. These data demonstrated that the COMM domain that defines this protein family serves as an interface for COMMD-COMMD interactions.

Several COMMD Proteins Suppress κB-mediated Transcription—MURR1/COMMD1, the prototype member of the family, was recently reported to inhibit κB-mediated transcription from endogenous and viral promoters (16). Therefore, the ability of other COMMD proteins to inhibit NF-κB was investigated. Cells were transfected with a κB-responsive reporter plasmid (2κB-luc) along with each of the COMMD proteins, and the response to TNF stimulation was subsequently evaluated. As shown in Fig. 4*A*, COMMD1, -2, -4, -7, -9, and -10 were capable of strongly inhibiting TNF-mediated NF-κB activation, whereas COMMD3 and -8 inhibited NF-κB weakly in this assay. Similarly, most COMMD proteins also inhibited basal levels of κB-mediated transcription.

Next, the ability of these proteins to control transcription of an endogenous κB-responsive gene was evaluated. Expression levels of endogenous *COMMD1*, *-4,* and *-6* were decreased by the use of RNA interference (RNAi), and the induction of *c-IAP2* mRNA levels in response to TNF was evaluated (Fig. 4, *B* and *C*). The effectiveness of RNAi against *COMMD1*, *-4*, and *-6* was confirmed by quantitative RT-PCR (Fig. 4*C*). When compared with mRNA levels present in control samples, transfection with siRNA oligonucleotides against *COMMD1*, *-4,* and *-6* resulted in a 75–95% suppression of mRNA expression, consistent with efficient RNAi of these transcripts. Next, the effect of reduced COMMD expression on *cIAP-2* transcription was evaluated (Fig. 4*B*). In cells transfected with oligonucleotides against an irrelevant target (GFP), treatment with TNF resulted in a 9-fold increase in *c-IAP2* mRNA levels, as measured by quantitative RT-PCR, a fold increase that is identical to that observed in untransfected cells (data not shown). Decreased *COMMD* levels resulted in heightened expression of *c-IAP2* after TNF treatment, with this effect being most notable after *COMMD6* RNAi. Therefore, these factors not only share a common domain but have similar functional properties in the regulation of NF-κB transcriptional activity.

COMMD Proteins Associate with the NF-κB Complex—The ability of COMMD1 to inhibit κB-mediated transcription was previously found to depend on its association with the NF-κB complex (16). Indeed, precipitation of endogenous COMMD1 with the use of rabbit polyclonal sera against COMMD1 resulted in the co-precipitation of endogenous RelA and c-Rel (Fig. 5*A*).

The possibility that other COMMD proteins can interact with the NF-κB complex was evaluated using fusion proteins with GST expressed in 293 cells. Precipitations with glutathione-Sepharose beads were performed followed by immunoblotting for detection of endogenous NF-κB subunits RelA, c-Rel, RelB, NF-κB1/p105, and NF-κB2/p100. As was the case for COMMD1, most COMMD proteins were also capable of precipitating NF-κB complexes (Fig. 5*B*). Although the intensity of recovery of NF-κB subunits correlated with the level of expression of the COMMD-GST proteins themselves (data not shown), the pattern of association with NF-κB subunits was different between the various COMMDs. Some COMMD proteins favor complexes containing RelB and NF-κB1/p105 (as in the case of COMMD3 and 9), whereas others seem to interact preferentially with RelA-containing complexes (as in the case of COMMD6 and -7). COMMD1, -2, -4, -5, -8, and -10 could associate more broadly with NF-κB subunits, although pattern differences were still evident. COMMD1 could asso-

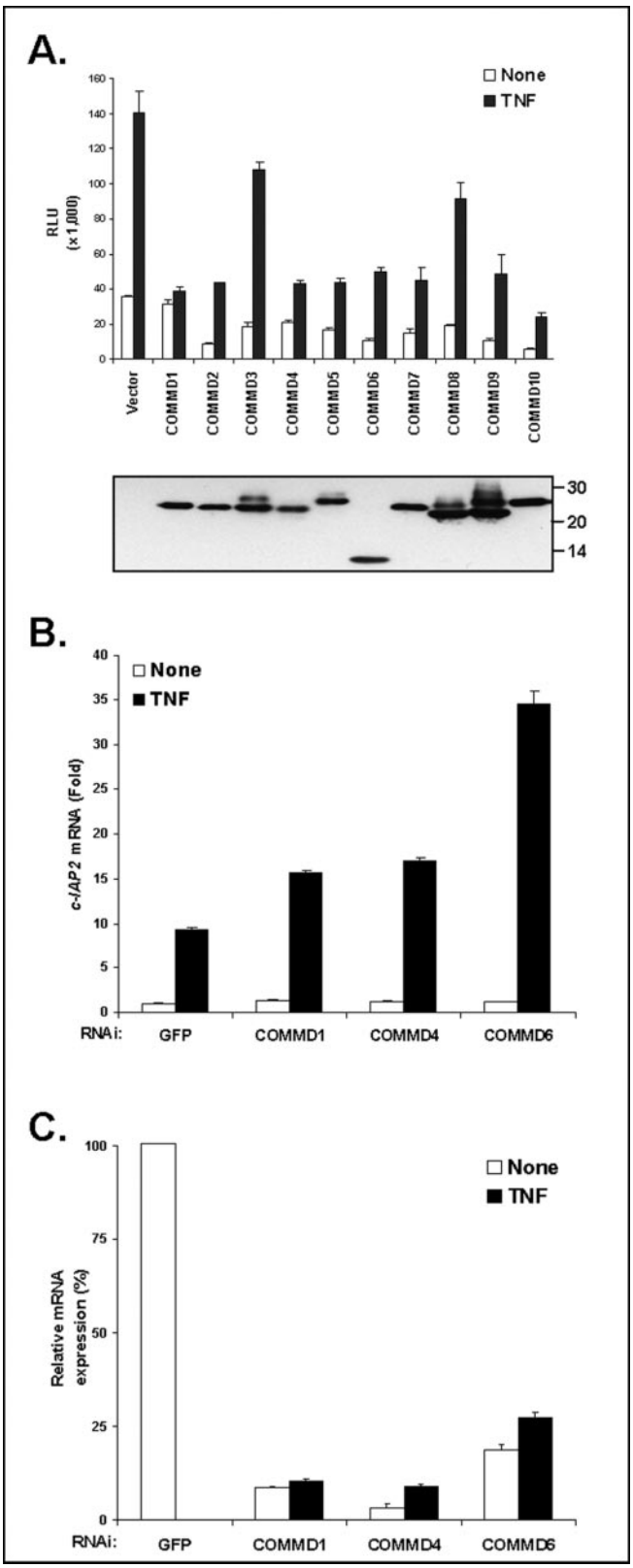

FIG. 4. *A*, COMMD proteins suppress κB-mediated transcription. Cells were transfected with the 2κB-luciferase reporter and COMMD proteins and were treated with TNF (1000 units/ml) for 12 h. Transcriptional activation of NF-κB was determined by luciferase assay (*top panel*), and expression of COMMD proteins in these lysates was determined by Flag immunoblotting (*bottom panel*). *RLU*, relative luminescence units. *B*, effect of COMMDs on *c-IAP2* expression. Endogenous levels of COMMD1, -4, and -6 were decreased with the use of siRNA oligonucleotides. The effects of TNF treatment on the expression levels of *c-IAP2*, a known NF-κB responsive gene, were evaluated by quantitative RT-PCR. *C*, efficiency of *COMMD* RNAi. Levels of expression of *COMMD1*, *-4,* and *-6* were determined by quantitative RT-PCR and compared with the corresponding control samples transfected with the GFP siRNA oligonucleotide. The data are presented as a percentage of the control samples, which was standardized to 100%.

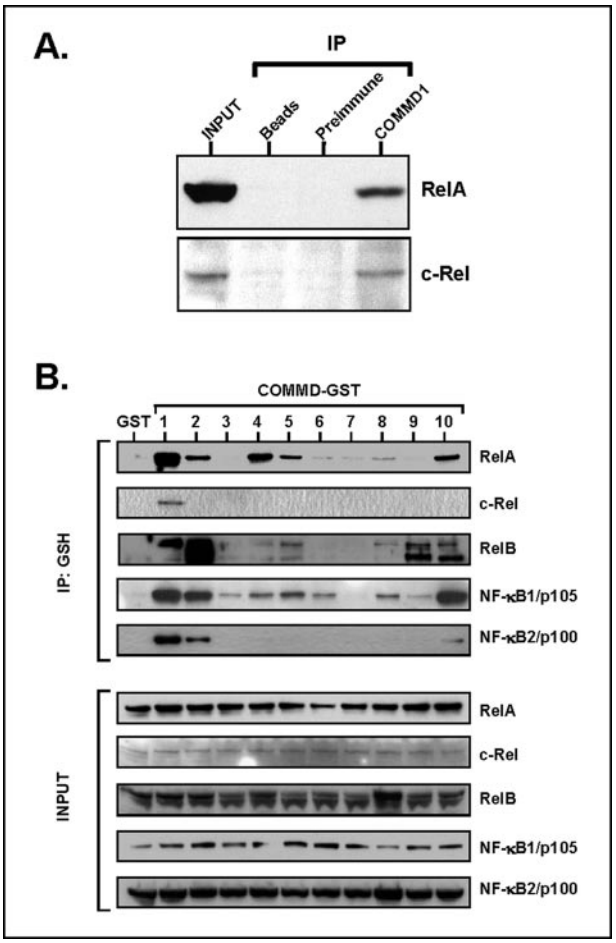

FIG. 5. *A*, COMMD1 associates with endogenous NF-κB subunits. Endogenous COMMD1 was immunoprecipitated (*IP*) from cell lysates prepared from 293 cells. This material was immunoblotted for endogenous RelA (*top panel*) and c-Rel (*bottom panel*). *B*, other COMMDs also associate with NF-κB. GST fusions with all COMMD proteins were expressed in 293 cells and precipitated from cell lysates by glutathione-Sepharose beads, and the presence in the precipitates of endogenous RelA, c-Rel, RelB, NF-κB1/p105, and NF-κB/p100 was determined by immunoblotting.

ciate with all five subunits and was the only COMMD able to precipitate c-Rel, whereasCOMMD2 also associated broadly with NF-κB subunits but interacted more strongly with RelB-containing complexes.

COMMD1-NF-κB Interactions Can Be Mapped to Distinct Domains—The ability of various regions of COMMD1 to sustain an interaction with endogenous RelA was evaluated next. In these experiments GST fusions of various domains of COMMD1, as depicted in Fig. 3*B*, were used for co-precipitation experiments. Unlike COMMD1-COMMD interactions that seem to require only the COMM domain (Fig. 3, *C* and *D*), COMMD1-RelA interactions are only detectable with full-length COMMD1 (Fig. 6*A*). Therefore, the interaction between COMMD1 and RelA relies on the presence of elements other than the COMM domain.

Next, the interaction between COMMD1 and RelA was evaluated further by determining the domains in RelA that are required for this interaction (Fig. 6*B*). Different domains of RelA in fusion with GST were expressed in 293 cells and

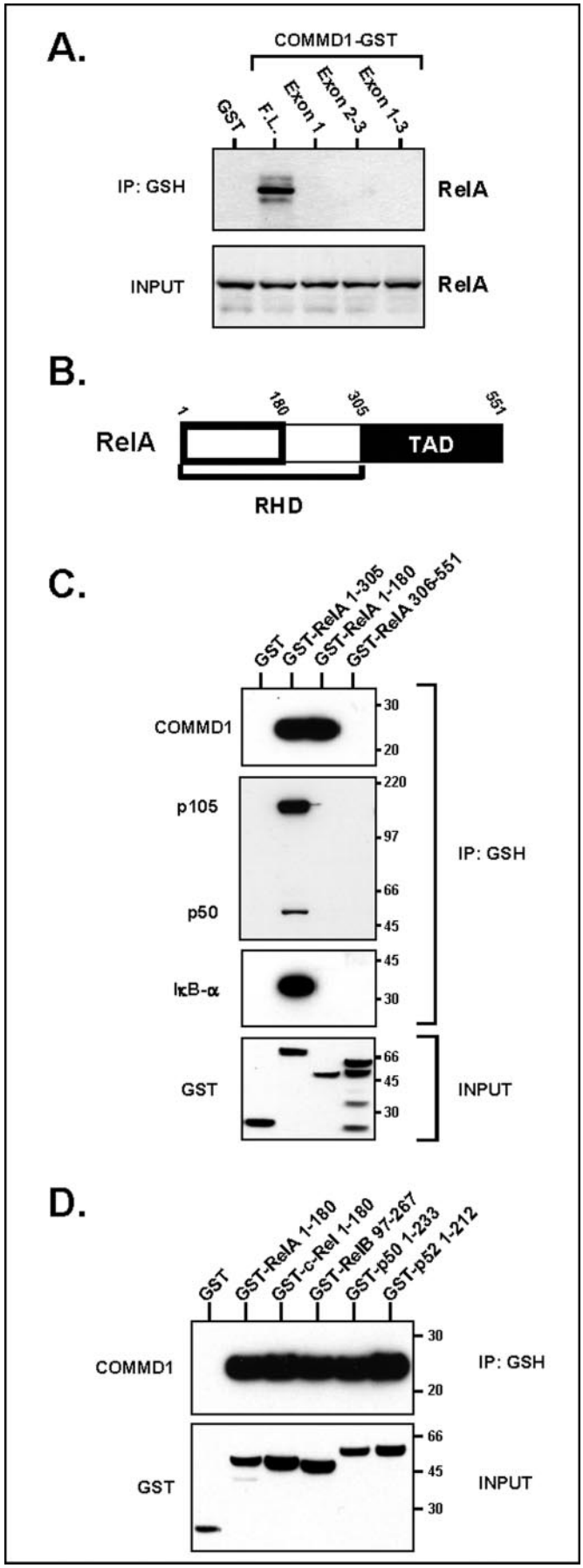

FIG. 6. *A*, domains involved in the interaction between COMMD1 and RelA. Deletion constructs of COMMD1 in fusion with GST corresponding to the boundaries described in Fig. 3*B* were utilized for co-precipitation experiments. The presence of endogenous RelA in the precipitate was determined by immunoblotting. *B*, shown is a schematic depicting the boundaries of the RHD and transactivation domain (*TAD*) of RelA. *C*, the ability of COMMD1 to bind to different regions of RelA was evaluated. Different domains of RelA were expressed in fusion with GST in 293 cells. These fusion proteins were precipitated from cell lysates by glutathione-Sepharose beads, and the presence of COMMD1, p50/p105, and IκB-α was determined by immunoblotting. Input levels for COMMD1, p50, p105, and IκB-α were identical in all samples (data not shown). *D*, regions derived from other NF-κB subunits that are homologous to RelA-(1–180) were expressed in fusion with GST and precipitated from cell lysates with glutathione-Sepharose beads. The presence of COMMD1 in the precipitate was determined by immunoblotting. Input levels for COMMD1 were identical in all samples (data not shown). *IP*, immunopreipitate.

precipitated with glutathione-Sepharose beads; the presence of COMMD1, p50 or its precursor p105, and IκB-α in the precipitates was determined by immunoblotting. As shown in Fig. 6*C*, the RHD of RelA was sufficient for binding to COMMD1, p50 or p105, and IκB-α. The carboxyl-terminal 246 amino acids of RelA (306–551), which correspond to the transactivation domain of the molecule (TAD), did not bind any of these molecules. Within the RHD, the first 180 amino acids comprise the DNA binding domain, whereas the remainder of the RHD (181–305) contains residues involved in IκB binding and dimerization with other subunits and the nuclear localization signal. Interestingly, the first 180 amino acids of RelA were capable of binding COMMD1 but not p50/p105 or IκB-α, probably because of the absence of the dimerization sequences. Reciprocal experiments, in which precipitation of COMMD1-GST was performed to determine its ability to bind to different domains of RelA, also supported these results (data not shown).

The RHD is highly conserved in all five NF-κB subunits (34). Therefore, the possibility that COMMD1 could also bind to similar sequences present in the RHD of other NF-κB subunits was similarly evaluated. Sequences contained in c-Rel-(1–180), RelB-(97–267), p50-(1–233), and p52-(1–212) were found to be homologous to RelA-(1–180) by aligning all five subunits using the ClustalV algorithm (data not shown). Each one of these regions in fusion with GST was expressed in 293 cells and precipitated from cell lysates with glutathione-Sepharose beads, and the presence of COMMD1 was determined by immunoblotting. As shown in Fig. 6*D*, these homologous regions, present in the RHD of all five NF-κB subunits, were capable of binding to COMMD1.

COMMD1 Does Not Affect Nuclear Translocation of NF-κB—In most cells NF-κB is ordinarily localized in the cytoplasm through interactions with members of the IκB family, which results in masking of the nuclear localization signal and cytoplasmic sequestration of the complex (11). Because the translocation of NF-κB from the cytosol to the nucleus is a well characterized regulatory step in the activation of κB-dependent transcription, the ability of COMMD1 to affect this process was investigated.

First, cellular localization of a fusion protein between RelA and EGFP was assessed by fluorescence microscopy before and after TNF treatment. TNF stimulation resulted in nuclear translocation of EGFP-RelA, a process that was inhibited in cells cotransfected with a superdominant form of IκB-α (Fig. 7, *A* and *B*). In contrast, the distribution of EGFP-RelA was unchanged by COMMD1 transfection, suggesting that unlike IκB-α, COMMD1 does not suppress the nuclear translocation of the NF-κB complex.

The translocation of NF-κB complexes into the nucleus and their DNA binding capacity was also evaluated by EMSA. Cells transfected with a control vector and subsequently treated with TNF demonstrated increased κB binding activity in nuclear extracts (Fig. 7*C*). As a control, this induction was blocked by

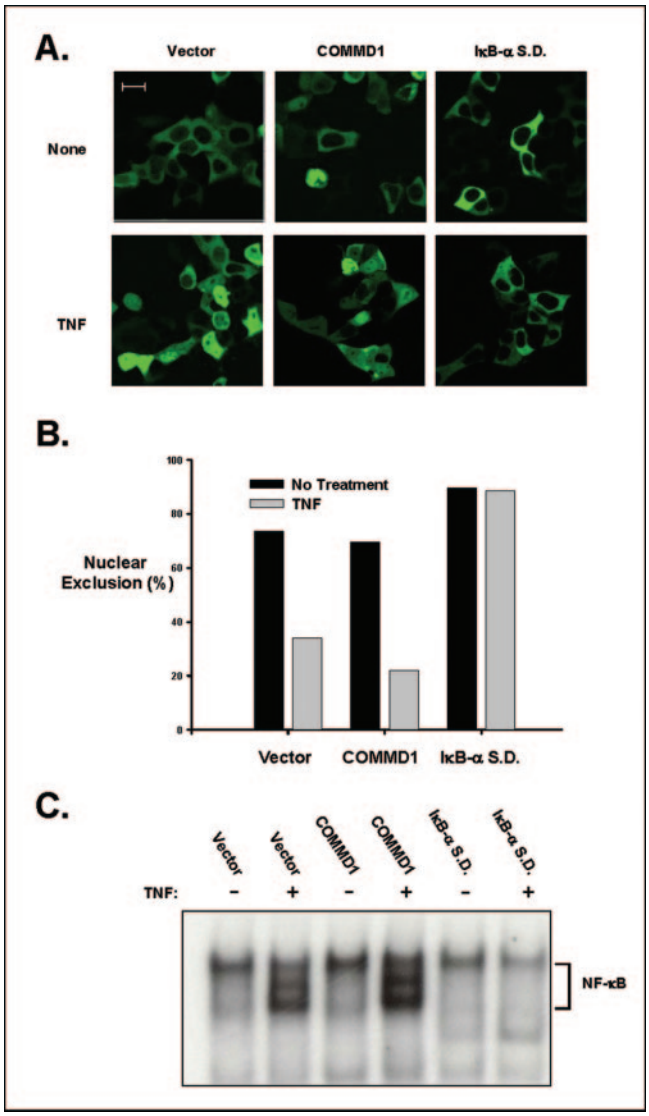

FIG. 7. *A*, COMMD1 does not prevent nuclear translocation of NF-κB. 293 cells were plated in cover glass-chambered slides and transfected with a vector encoding for RelA in fusion with EGFP and with COMMD1, IκB-αS.D. or a vector control (pEBB). Twenty-four hours after transfection cells were treated with TNF for 1 h. Representative images are shown (magnification bar corresponds to 18 μm). *B*, quantification of nuclear translocation. 293 cells were plated 6-well dishes, transfected as described in *A* and treated with TNF for 1 h. Before and after treatment, 250–400 cells in each group were counted under the microscope and rated for the presence or absence of appreciable nuclear signal from RelA, the absence of which was recorded as nuclear exclusion. The data are presented as a percentage of the total number of cells counted in each group. *C*, nuclear translocation was also evaluated by EMSA. 293 cells plated in 10-cm plates were transfected with the constructs indicated in the figure. TNF stimulation was performed 30 min before extraction of nuclear proteins, which were used for EMSA.

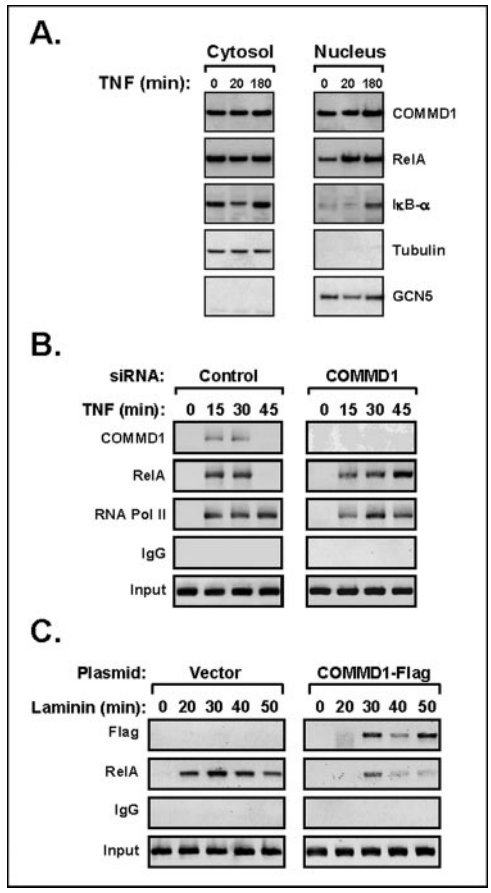

FIG. 8. *A*, presence of a nuclear pool of COMMD1. Cell lysates were fractionated to obtain nuclear and cytosolic fractions during timed stimulation with TNF. These fractions were used for immunoblotting to determine the cellular localization of endogenous COMMD1. As a control for the of TNF stimulation, the effects on RelA and IκB-α levels were also determined by immunoblotting. Tubulin and GCN5 served as cytosolic and nuclear markers, respectively. *B* and *C*, COMMD1 inhibits chromatin occupancy by NF-κB. ChIP analysis on the *cIAP-2* promoter after TNF stimulation was performed on DU145 cells transfected with siRNA oligonucleotides to COMMD1 or GFP (control). (*B*). ChIP analysis was performed on the *cIAP-2* gene using 293 cells expressing either Flag-tagged COMMD1 or empty vector control. Cell adhesion to a laminin-coated plate was used as the NF-κB activating stimulus. *Pol*, polymerase.

transfection of superdominant IκB-α. However, COMMD1 transfection had no appreciable effects on the induction of κB binding activity in nuclear extracts after TNF treatment. In addition, whereas RNAi of COMMD1 led to transcriptional activation of NF-κB, this did not lead to induction of κB binding by EMSA (data not shown).

COMMD1 Binds to κB-responsive Promoter Regions and Affects NF-κB Binding to Chromatin—Although COMMD proteins can interact with the NF-κB complex, the ability of COMMD1 to inhibit transcriptional activation is independent of the nuclear translocation of NF-κB. This suggested that the activity of NF-κB complexes in the nucleus was compromised by COMMD1. To investigate this possibility, the presence of nuclear COMMD1 was first established. Subcellular fractions were prepared from 293 cells during timed stimulation with TNF (including an early and late time point). As shown in Fig. 8*A*, COMMD1 was present in both nuclear and cytosolic fractions, and its quantity seemed slightly increased in the late time point (180 min). As expected, TNF stimulation also resulted in nuclear translocation of RelA and early degradation of IκB-α with late accumulation of this protein in the nuclear fraction. The purity of the fractions was determined by immunoblotting for tubulin (cytosolic marker) and GCN5 (nuclear marker).

Based on the above findings, the effects of COMMD1 on NF-κB nuclear function were investigated by examining the recruitment of RelA to chromatin. Utilizing ChIP, the effects of COMMD1 levels on the recruitment of RelA to the κB-responsive *c-IAP2* promoter were determined. The effects of stimulation with TNF were compared after transfection of control and COMMD1 siRNA oligonucleotides (Fig. 8*B*). Decreases in endogenous COMMD1 levels resulted in prolongation of the occupancy time of RelA on the *c-IAP2* promoter. In addition, COMMD1 itself was found to be recruited to this κB-responsive site after TNF stimulation. A complementary set of experiments was also performed to determine if increases in

COMMD1 protein levels would have the converse effect on RelA recruitment to chromatin. In this case, cell adhesion to laminin was used as the stimulus for NF-κB activation, as this results in robust and sustained recruitment of RelA to the *c-IAP2* promoter site. As shown in Fig. 8*C*, overexpression of COMMD1 resulted in a marked decrease in the duration of RelA association with chromatin after NF-κB activation; again, COMMD1 recruitment to chromatin in response to stimulation was also detected.

Taken together, these data indicate that COMMD1 affects the half-life of the RelA-chromatin complex that is recruited in response to NF-κB-activating stimuli. Because COMMD1 itself is recruited to chromatin and remains associated even after NF-κB has been displaced, this suggests that COMMD1 either alone or through the recruitment of other factors can affect the affinity of NF-κB for chromatin.

DISCUSSION

In this report we describe the identification of a novel and conserved family of homologs of MURR1. These factors are defined by the presence of a unique carboxyl-terminal motif termed the COMM domain. The existence of this protein family and any insights into the cellular functions of these factors were largely unknown up to this point.

We show here that all COMMD proteins can interact with MURR1/COMMD1. Interestingly, whereas all 10 factors are expressed in 293 cells, only COMMD3, -4, and -6 were identified as COMMD1-associated factors in our TAP screen, suggesting that certain associations might be preferentially present in cells. In addition, other COMMD-COMMD complexes that do not include COMMD1 are likely to occur, and indeed, our search of the *Drosophila* protein interaction map recently published (35) predicts an interaction between *Drosophila* COMMD2 and COMMD3. Therefore, once antibodies to all 10 proteins are available, the composition of physiologic COMMD-COMMD complexes would be able to be identified. We also show that interactions between COMMD proteins are mediated by the COMM domain.

Several COMMD proteins are functionally similar to the prototype member of the family, MURR1/COMMD1, and bind to and suppress NF-κB. We studied in further detail the binding mechanism by which COMMD1 interacts with RelA and demonstrate that this is distinct from dimerization to other NF-κB subunits or binding to IκB-α (Fig. 6*C*), indicating that these two events are not required for the interaction of COMMD1 with NF-κB. This is similarly supported by the observation that COMMDs can also associate with RelB (Fig. 5*B*), an NF-κB subunit that does not associate with IκB-α (36). These findings suggest that the prior identification of an association between IκB-α and COMMD1 that requires the ankyrin repeats of IκB-α could be potentially explained as a tertiary complex, since the ankyrin repeats are required for IκB-α binding to the NF-κB subunits (16).

Unlike the association between COMMD1 and itself or COMMD3, COMMD1-RelA interactions are not supported by the COMM domain alone (Figs. 3, *C* and *D*, and 6*A*), indicating that the association of COMMDs to NF-κB complexes is likely mediated by a mechanism distinct from COMMD-COMMD interaction. Similarly, the pattern of COMMD association to NF-κB could not be simply explained by COMMD multimer formation. Despite the demonstrated interaction between COMMD1 and COMMD3, only COMMD1 could precipitate RelA. In addition, COMMD9 could readily precipitate RelB, whereas COMMD6 did not despite the stronger COMMD6-COMMD1 interaction (Figs. 3*A* and 5*B*).

NF-κB-mediated transcription is largely controlled by the cytoplasmic sequestration of NF-κB complexes through the binding to ankyrin repeat-containing inhibitory molecules such as the IκBs (11, 37). Activation of the IκB kinase complex in response to a variety of extracellular signals initiates a cascade of events leading to IκB degradation and nuclear translocation on NF-κB. Whereas a role for MURR1/COMMD1 in the regulation of IκB-α degradation has been demonstrated (16), our findings here suggest that this effect is not sufficient to explain its ability to inhibit NF-κB-mediated transcription, since nuclear translocation of NF-κB subunits is unaffected by COMMD1. Rather, we find that COMMD1 can regulate the nuclear function of NF-κB through its recruitment to κB-responsive promoters where it affects the duration of RelA binding to chromatin.

Once activated, NF-κB can mediate expression of multiple gene targets. However, the observed responses are often specific to the cell type and stimulus in question. For example, NF-κB has been reported to be able to activate transcription of both pro- and anti-apoptotic factors in various settings (5, 6). The regulation of NF-κB solely by IκB-mediated sequestration of the complex is unlikely to account for these differences in gene expression. In this regard, post-translational modifications of NF-κB (38) and preferential promoter binding by different subunits have been shown to participate in the regulation of certain promoters in response to specific stimuli (36, 39). However, additional layers of regulation that could account for the tissue- and promoter-specific nature of the response are likely at play. The identification here of the COMMD family reveals an additional regulatory level that might be important in this regard. The conservation of all 10 *COMMD* genes through vertebrate evolution and the differential pattern of association to NF-κB complexes suggest that despite their similarities, COMMD proteins probably serve unique and non-redundant functions. A thorough understanding of the mode of action of these factors in different cell types may help to account for the precision and selectivity by which expression of the multitude of NF-κB-responsive genes can be orchestrated in response to a diverse range of stimuli.

Unlike other nuclear regulators of NF-κB such as histone acetylases and deacetylases, the COMMDs themselves possess no apparent intrinsic enzymatic activity. The transcriptional inhibitory functions of the COMMDs must in turn be regulated in response to certain stimuli, possibly by post-translational modifications. XIAP, a stress responsive pro-survival factor (40), can ubiquitinate COMMD1, resulting in its degradation (19), suggesting that the regulation of COMMD proteins might be integrated into cellular stress responses that are known to activate NF-κB.

Acknowledgments—We are grateful to B. Balliu for valuable technical assistance. We thank Dr. Neil Perkins for insightful suggestions and for generously providing several expression plasmids used in our studies. We are also indebted to Dr. Ranier de Martin who provided us with EGFP-p65.

REFERENCES

1. Ghosh, S., May, M. J., and Kopp, E. B. (1998) *Annu. Rev. Immunol.* **16,** 225–260
2. Silverman, N., and Maniatis, T. (2001) *Genes Dev.* **15,** 2321–2342
3. Karin, M., Yamamoto, Y., and Wang, Q. M. (2004) *Nat. Rev. Drug Discov.* **3,** 17–26
4. Joyce, D., Albanese, C., Steer, J., Fu, M., Bouzahzah, B., and Pestell, R. G. (2001) *Cytokine Growth Factor Rev.* **12,** 73–90
5. Karin, M., and Lin, A. (2002) *Nat. Immunol.* **3,** 221–227
6. Baldwin, A. S. (2001) *J. Clin. Investig.* **107,** 241–246
7. Perkins, N. D., Edwards, N. L., Duckett, C. S., Agranoff, A. B., Schmid, R. M., and Nabel, G. J. (1993) *EMBO J.* **12,** 3551–3558
8. Alcami, J., Lain de Lera, T., Folgueira, L., Pedraza, M. A., Jacque, J. M., Bachelerie, F., Noriega, A. R., Hay, R. T., Harrich, D., and Gaynor, R. B. (1995) *EMBO J.* **14,** 1552–1560
9. Nabel, G. J., and Baltimore, D. (1987) *Nature* **326,** 711–713
10. Bohnlein, E., Lowenthal, J. W., Siekevitz, M., Ballard, D. W., Franza, B. R., and Greene, W. C. (1988) *Cell* **53,** 827–836
11. Baldwin, A. S. (1996) *Annu. Rev. Immunol.* **14,** 649–681

12. Chen, Z., Hagler, J., Palombella, V. J., Melandri, F., Scherer, D., Ballard, D., and Maniatis, T. (1995) *Genes Dev.* **9,** 1586–1597
13. Greene, W. C. (2004) *Nat. Immunol.* **5,** 18–19
14. van De Sluis, B., Rothuizen, J., Pearson, P. L., van Oost, B. A., and Wijmenga, C. (2002) *Hum. Mol. Genet.* **11,** 165–173
15. Tao, T. Y., Liu, F., Klomp, L., Wijmenga, C., and Gitlin, J. D. (2003) *J. Biol. Chem.* **278,** 41593–41596
16. Ganesh, L., Burstein, E., Guha-Niyogi, A., Louder, M. K., Mascola, J. R., Klomp, L. W., Wijmenga, C., Duckett, C. S., and Nabel, G. J. (2003) *Nature* **426,** 853–857
17. Duckett, C. S., Li, F., Wang, Y., Tomaselli, K. J., Thompson, C. B., and Armstrong, R. C. (1998) *Mol. Cell. Biol.* **18,** 608–615
18. Richter, B. W. M., Mir, S. S., Eiben, L. J., Lewis, J., Reffey, S. B., Frattini, A., Tian, L., Frank, S., Youle, R. J., Nelson, D. L., Notarangelo, L. D., Vezzoni, P., Fearnhead, H. O., and Duckett, C. S. (2001) *Mol. Cell. Biol.* **21,** 4292–4301
19. Burstein, E., Ganesh, L., Dick, R. D., van De Sluis, B., Wilkinson, J. C., Lewis, J., Klomp, L. W. J., Wijmenga, C., Brewer, G. J., Nabel, G. J., and Duckett, C. S. (2004) *EMBO J.* **23,** 244–254
20. Duckett, C. S., Gedrich, R. W., Gilfillan, M. C., and Thompson, C. B. (1997) *Mol. Cell. Biol.* **17,** 1535–1542
21. Schmid, J. A., Birbach, A., Hofer-Warbinek, R., Pengg, M., Burner, U., Furtmuller, P. G., Binder, B. R., and de Martin, R. (2000) *J. Biol. Chem.* **275,** 17035–17042
22. Mir, S. S., Richter, B. W. M., and Duckett, C. S. (2000) *Blood* **15,** 4307–4312
23. Puig, O., Caspary, F., Rigaut, G., Rutz, B., Bouveret, E., Bragado-Nilsson, E., Wilm, M., and Seraphin, B. (2001) *Methods* **24,** 218–229
24. Duckett, C. S., Perkins, N. D., Kowalik, T. F., Schmid, R. M., Huang, E. S., Baldwin, A. S., Jr., and Nabel, G. J. (1993) *Mol. Cell. Biol.* **13,** 1315–1322
25. Birkey Reffey, S., Wurthner, J. U., Parks, W. T., Roberts, A. B., and Duckett, C. S. (2001) *J. Biol. Chem.* **276,** 26542–26549
26. Su, A. I., Wiltshire, T., Batalov, S., Lapp, H., Ching, K. A., Block, D., Zhang, J., Soden, R., Hayakawa, M., Kreiman, G., Cooke, M. P., Walker, J. R., and Hogenesch, J. B. (2004) *Proc. Natl. Acad. Sci. U. S. A.* **101,** 6062–6067
27. Hoberg, J. E., Yeung, F., and Mayo, M. W. (2004) *Mol. Cell* **16,** 245–255
28. Yeung, F., Hoberg, J. E., Ramsey, C. S., Keller, M. D., Jones, D. R., Frye, R. A., and Mayo, M. W. (2004) *EMBO J.* **23,** 2369–2380
29. Nabetani, A., Hatada, I., Morisaki, H., Oshimura, M., and Mukai, T. (1997) *Mol. Cell. Biol.* **17,** 789–798
30. Solban, N., Jia, H. P., Richard, S., Tremblay, S., Devlin, A. M., Peng, J., Gossard, F., Guo, D. F., Morel, G., Hamet, P., Lewanczuk, R., and Tremblay, J. (2000) *J. Biol. Chem.* **275,** 32234–32243
31. Semenova, E., Wang, X., Jablonski, M. M., Levorse, J., and Tilghman, S. M. (2003) *Hum. Mol. Genet.* **12,** 1301–1312
32. Haupt, Y., Barri, G., and Adams, J. M. (1992) *Mol. Biol. Rep.* **17,** 17–20
33. Roperch, J. P., Lethrone, F., Prieur, S., Piouffre, L., Israeli, D., Tuynder, M., Nemani, M., Pasturaud, P., Gendron, M. C., Dausset, J., Oren, M., Amson, R. B., and Telerman, A. (1999) *Proc. Natl. Acad. Sci. U. S. A.* **96,** 8070–8073
34. Chen, F. E., Huang, D. B., Chen, Y. Q., and Ghosh, G. (1998) *Nature* **391,** 410–413
35. Giot, L., Bader, J. S., Brouwer, C., Chaudhuri, A., Kuang, B., Li, Y., Hao, Y. L., Ooi, C. E., Godwin, B., Vitols, E., Vijayadamodar, G., Pochart, P., Machineni, H., Welsh, M., Kong, Y., Zerhusen, B., Malcolm, R., Varrone, Z., Collis, A., Minto, M., Burgess, S., McDaniel, L., Stimpson, E., Spriggs, F., Williams, J., Neurath, K., Ioime, N., Agee, M., Voss, E., Furtak, K., Renzulli, R., Aanensen, N., Carrolla, S., Bickelhaupt, E., Lazovatsky, Y., DaSilva, A., Zhong, J., Stanyon, C. A., Finley, R. L., Jr., White, K. P., Braverman, M., Jarvie, T., Gold, S., Leach, M., Knight, J., Shimkets, R. A., McKenna, M. P., Chant, J., and Rothberg, J. M. (2003) *Science* **302,** 1727–1736
36. Saccani, S., Pantano, S., and Natoli, G. (2003) *Mol. Cell* **11,** 1563–1574
37. Henkel, T., Machleidt, T., Alkalay, I., Krönke, M., Ben-Neriah, Y., and Baeuerle, P. A. (1993) *Nature* **365,** 182–185
38. Vermeulen, L., De Wilde, G., Notebaert, S., Vanden Berghe, W., and Haegeman, G. (2002) *Biochem. Pharmacol.* **64,** 963–970
39. Bonizzi, G., Bebien, M., Otero, D. C., Johnson-Vroom, K. E., Cao, Y., Vu, D., Jegga, A. G., Aronow, B. J., Ghosh, G., Rickert, R. C., and Karin, M. (2004) *EMBO J.* **23,** 4202–4210
40. Holcik, M., and Korneluk, R. G. (2001) *Nat. Rev. Mol. Cell Biol.* **2,** 550–556